A unified energy-optimality criterion predicts human navigation paths and speeds

Geoffrey L. Brown[a,b,1], Nidhi Seethapathi[a,c,1], and Manoj Srinivasan[a,d,2]

[a]Mechanical and Aerospace Engineering, The Ohio State University, Columbus, OH 43210; [b]Feinberg School of Medicine, Northwestern University, Chicago, IL 60611; [c]Department of Bioengineering, University of Pennsylvania, Philadelphia, PA 19104; and [d]Program in Biophysics, The Ohio State University, Columbus, OH 43210

Edited by Andrew A. Biewener, Harvard University, Bedford, MA, and accepted by Editorial Board Member C. O. Lovejoy May 9, 2021 (received for review October 5, 2020)

Navigating our physical environment requires changing directions and turning. Despite its ecological importance, we do not have a unified theoretical account of non-straight-line human movement. Here, we present a unified optimality criterion that predicts disparate non-straight-line walking phenomena, with straight-line walking as a special case. We first characterized the metabolic cost of turning, deriving the cost landscape as a function of turning radius and rate. We then generalized this cost landscape to arbitrarily complex trajectories, allowing the velocity direction to deviate from body orientation (holonomic walking). We used this generalized optimality criterion to mathematically predict movement patterns in multiple contexts of varying complexity: walking on prescribed paths, turning in place, navigating an angled corridor, navigating freely with end-point constraints, walking through doors, and navigating around obstacles. In these tasks, humans moved at speeds and paths predicted by our optimality criterion, slowing down to turn and never using sharp turns. We show that the shortest path between two points is, counterintuitively, often not energy-optimal, and, indeed, humans do not use the shortest path in such cases. Thus, we have obtained a unified theoretical account that predicts human walking paths and speeds in diverse contexts. Our model focuses on walking in healthy adults; future work could generalize this model to other human populations, other animals, and other locomotor tasks.

optimization | locomotion | human movement | predictive theory | metabolic energy

Real-world human navigation through our physical environment requires changing direction and turning, maneuvering around obstacles, and moving along complex paths. In one previous study that tracked indoor locomotion over many days, 35 to 45% of steps required turns (1). Despite the importance of turning in ecological settings, we do not have a coherent theoretical account of the paths and speeds observed in such locomotion. Human-subject experiments (2–7) and mathematical models (5, 8–15) have suggested that energy optimality explains many aspects of straight-line locomotion, at least approximately. However, we do not know if such energy optimality generalizes to walking while navigating a more complex environment. Here, we obtain a better understanding of locomotion with turning, first quantifying its increased energetic demands and then showing that accounting for these increased energetic demands correctly predicts human navigation paths and speeds in a variety of naturalistic locomotor contexts.

Over the years, researchers have measured human locomotion in a few contexts requiring changing direction—for instance, navigating through angled corridors (16), moving from point to point while having to turn (17), walking through doors, and avoiding obstacles (18, 19). However, previous models aimed at explaining such data used minimization principles that were not physiologically based, required fitting model parameters to behavioral data, were generally fit to only one experiment, and did not generalize to multiple experiments (17–19). As we argue later on, these models could not simultaneously explain the paths and speeds observed in curvilinear walking, often predicting zero speeds for simple tasks. Here, we provide a theoretical account that does not have these limitations and is broadly predictive.

We perform human-subject experiments to quantify the metabolic cost of humans walking with turning, measuring how the metabolic cost increases with walking speed and the turning rate. We generalize this empirically derived metabolic-cost landscape to walking along arbitrary paths and then use an optimization-based framework to make a number of behavioral predictions about humans walking in tasks of different complexity. We compared our predictions to five different experiments, each containing a qualitatively different walking or turning task. These five experiments consisted of two behavioral experiments that we performed here and data from three prior studies. Specifically, we predict that humans would walk slower when turning in smaller circles, which we compare with our own behavioral experiments, correctly predicting the lowered walking speeds. We show that the speed at which humans turn in place is approximately predicted by minimizing the cost of turning, again comparing with our own experiments. Finally, minimizing the same metabolic model, we predict more complex walking behavior involving navigation observed in three previous studies: walking freely from point to point (17), walking through doors and avoiding obstacles (18, 19), and walking and turning along an angled corridor (16). We show that energy optimality explains many qualitative and quantitative features of human walking,

Significance

Why do humans move the way they do? Here, we obtain a physiologically based theory of the speeds and paths with which humans navigate their environment. We measure the metabolic energy cost of walking with turning and show that minimizing this cost explains diverse phenomena involving navigating around obstacles, walking in complex paths, and turning. We explain why humans slow down while turning, avoid sharp turns, do not always use the shortest path, and other naturalistic locomotor phenomena.

Author contributions: G.L.B., N.S., and M.S. designed research; G.L.B., N.S., and M.S. performed research; G.L.B., N.S., and M.S. contributed new reagents/analytic tools; G.L.B., N.S., and M.S. analyzed data; G.L.B., N.S., and M.S. wrote the paper; and M.S. supervised research and obtained funding.

The authors declare no competing interest.

This article is a PNAS Direct Submission. A.A.B. is a guest editor invited by the Editorial Board.

[1]G.L.B. and N.S. contributed equally to this work.

[2]To whom correspondence may be addressed. Email: srinivasan.88@osu.edu.

This article contains supporting information online at https://www.pnas.org/lookup/suppl/doi:10.1073/pnas.2020327118/-/DCSupplemental.

Published July 15, 2021.

including not taking sharp turns, path shapes adopted while walking with turning, and speed reductions during turns, as observed in these prior experimental studies (16–19), but heretofore not predicted by a single theoretical model. Both our metabolic models and behavioral predictions focus on walking in healthy adults, and we outline the benefits of generalizing our approach to other populations and other locomotor tasks.

Results

Turning Increases Metabolic Cost Substantially. We measured the metabolic energy expenditure of 17 human subjects while walking with turning. To measure the cost of turning, we instructed the subjects to walk in circles of different radii and at different tangential speeds along the circle. We provided feedback to them to ensure that they were able to perform the required task (Fig. 1*A* and *Materials and Methods*). Each subject performed at least 16 trials of four radii and at least four speeds. We measured metabolic energy expenditure using indirect calorimetry—that is, by tracking respiratory oxygen and carbon dioxide flux (20). Fig. 1*B* shows the resulting mass-normalized metabolic rate—that is, metabolic energy per unit time per unit subject mass $\dot{E}$—as a function of prescribed speed v and path radius R. These measurements show that for a given prescribed walking speed, the metabolic energy expenditure was higher for smaller radii or, equivalently, for higher path curvature (Fig. 1). For instance, directly comparing the measured metabolic rates at equal prescribed speeds, but different radii, we find that walking at a 1-m radius was more expensive than walking at a 4-m radius by 0.59 W/kg on average ($p < 4 \times 10^{-4}$ using a right-tailed t test), a 1-m radius was more expensive than a 2-m radius by 0.46 W/kg on average ($p = 9 \times 10^{-4}$), and a 2-m radius was more expensive than a 4-m radius by 0.14 W/kg on average ($p < 10^{-6}$). These differences constitute large energy penalties relative to the resting metabolic rate: 40%, 20%, and 10%, respectively, corresponding to Cohen's d effect sizes of 0.64, 0.62, and 0.15. Because these differences are computed at matched speeds (albeit prescribed speeds), the differences are significant for both metabolic cost per unit time and per unit distance around the circle.

Metabolic Rate Increases Nonlinearly with Linear and Angular Speeds. The total metabolic rate was described well by the following quadratic function of the linear speed v (tangent to the walking path) and the angular speed $\omega = v/R$ as follows (Fig. 1*B*):

$$\dot{E} = \alpha_0 + \alpha_1 v^2 + \alpha_2 \frac{v^2}{R^2} = \alpha_0 + \alpha_1 v^2 + \alpha_2 \omega^2, \qquad [1]$$

with $\alpha_0 = 2.204 \pm 0.079$ W/kg, $\alpha_1 = 1.213 \pm 0.054$ W/kg/$(\mathrm{ms}^{-1})^2$, and $\alpha_2 = 0.966 \pm 0.061$ W/kg/$(\mathrm{rad} \cdot \mathrm{s}^{-1})^2$, giving the metabolic rate $\dot{E}$ in W/kg (normalized by body mass), where v is in ms^{-1}, R is in meters, and ω is in $\mathrm{rad \cdot s}^{-1}$. The p values for the three coefficients obeyed $p < 10^{-30}$, compared to a null constant model of zero coefficients. Eq. **1** explains 88.1% of the empirical metabolic-rate variance over all subjects (this percentage is the statistical R-squared value, the coefficient of determination, not to be confused with radius-squared).

The form for the metabolic-rate expression in Eq. **1** was chosen in analogy to classic work on straight-line walking (2, 21), which found that the metabolic rate is close to linear in v^2—that is, $\dot{E} \sim \alpha_0 + \alpha_1 v^2$. In a post hoc analysis, we compared the 88.1% variance explained by simple quadratic expression in Eq. **1** to more general quadratic expressions for $\dot{E}$ (with additional $v, |\omega|$ and $v|\omega|$ terms); such more general quadratic expressions increased the explained variance by less than 0.7% (*SI Appendix*, Table S1). We used the absolute value $|\omega|$, as we did not distinguish between leftward and rightward turns, ignoring any left–right gait asymmetries. Among such more general quadratic models, the model in Eq. **1** has the lowest Bayesian Information Criterion, a common model-selection criterion that promotes model parsimony

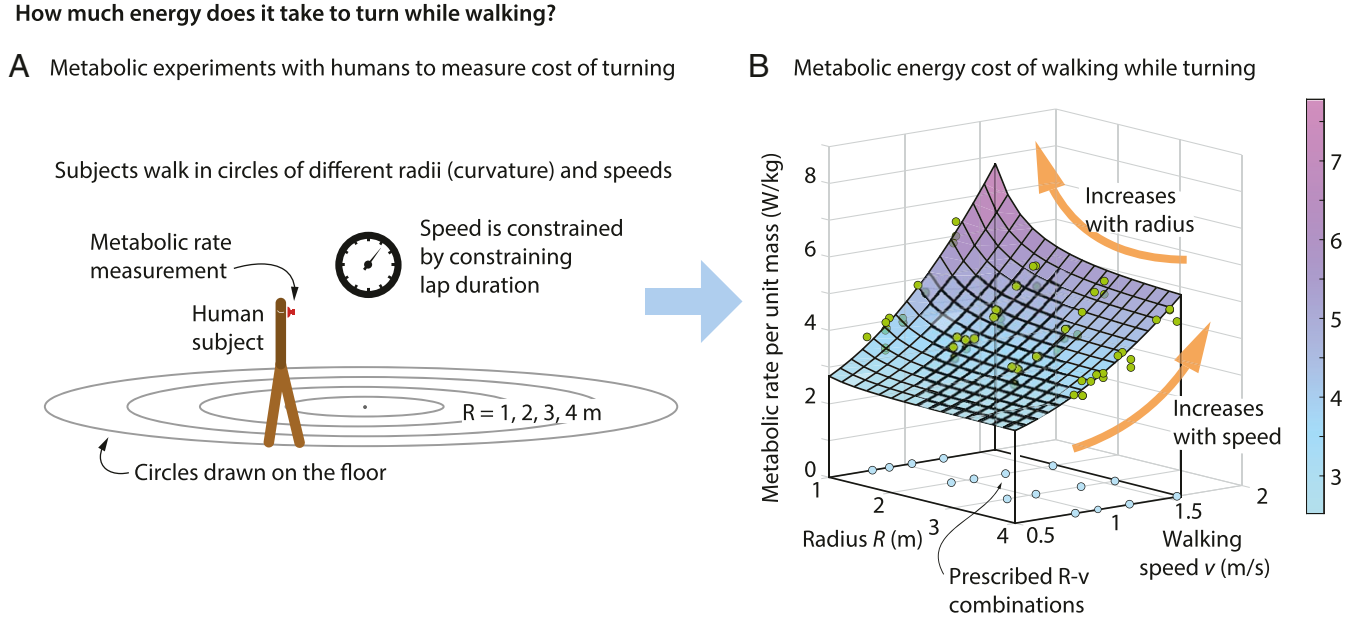

Fig. 1. Energy-cost landscape of turning from humans walking in circles. (*A*) We estimated the metabolic rate as a function of walking speed and turning radius by having subjects walk in circles of a few different radii and at a few different speeds at each radius. Speeds were constrained by having them complete laps at prescribed durations. Metabolic rate was estimated by using respiratory-gas analysis. (*B*) The metabolic-rate data per unit body mass ($\dot{E}$) is higher for higher speeds and lower radii. The prescribed speeds and radii (v, R) at which the data were collected are shown as blue dots on the horizontal plane ($\dot{E} = 0$ plane); raw metabolic data points from four representative subjects are shown as green dots (see Dataset S1 for all data). The wireframe surface shows the best-fit model $\dot{E} = \alpha_0 + \alpha_1 v^2 + \alpha_2 \omega^2$, capturing the nonlinear increase with both linear velocity v and angular velocity ω; the model captures 88.1% of the data variance. The four corners of the cost surface have been connected to the horizontal plane to enhance the 3D visualization; a contour plot version of this surface is in *SI Appendix*, Fig. S1.

while maintaining a good fit to data (22). Similarly, allowing exponents other than two in the model expression, considering $\dot{E} \sim \alpha_0 + \alpha_1 v^{\gamma} + \alpha_2 \omega^{\delta}$, improves the explained variance by less than 0.4% while adding two more model parameters, and so we did not consider it further.

Straight-Line Walking Is a Less Expensive Special Case. Setting angular speed ω to zero or radius R to infinity in Eq. **1** gives $\dot{E}$ for straight-line walking: $\alpha_0 + \alpha_1 v^2$. Thus, as noted, the quadratic expression (Eq. **1**) generalizes the classic quadratic expression for the straight-line-walking metabolic rate, namely, $\alpha_0 + \alpha_1 v^2$ (2). Previous studies of overground or treadmill straight-line walking (2, 4) have estimated $\alpha_0 \approx 2 - 2.5$ W/kg and $\alpha_1 \approx 0.9 - 1.4$ W/(kg·ms^{-1}), and our estimates are squarely in this same range. Because the coefficient $\alpha_2 > 0$ with $p < 10^{-4}$, the model (Eq. **1**) confirms that the estimated metabolic rate is higher for lower radii R for a given tangential speed v. This radius dependence implies, for instance, that at speed $v = 1.5$ m/s, reducing the radius R from infinity to 1 m induces an additional cost ($\alpha_2 v^2/R^2$) of about 43% of the total straight-line-walking metabolic rate ($\alpha_0 + \alpha_1 v^2$). This turning cost is about 60% of the net straight-line-walking metabolic rate ($\alpha_0 + \alpha_1 v^2 - \dot{E}_{\mathrm{rest}}$)—that is, over and above the resting metabolic rate $\dot{E}_{\mathrm{rest}}$.

As a brief aside, we note that the coefficient α_0 has the interpretation of the metabolic rate of walking steadily at very low speeds ($v \approx 0$), which is substantially higher than, and should not be conflated with, the resting metabolic rate $\dot{E}_{\mathrm{rest}}$ (here, around 1.4 W/kg). This difference between α_0 and $\dot{E}_{\mathrm{rest}}$ is similar to differences found by previous studies between the cost of standing still and very slow walking with stepping (2).

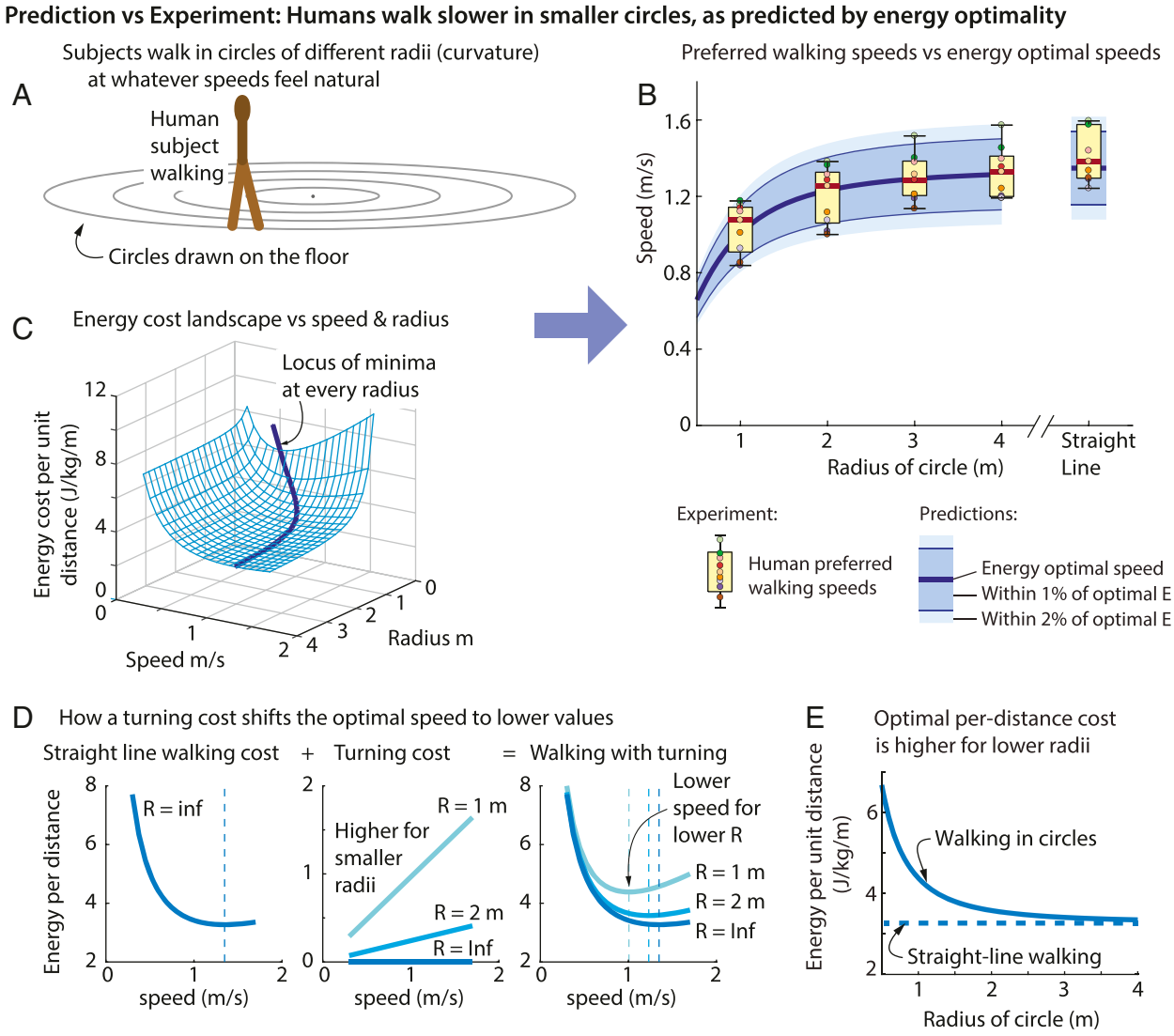

Fig. 2. Prediction vs. behavior: preferred walking in circles. (*A*) To test behavioral predictions of energy-optimal walking, we asked subjects to walk on circles of different radii at whatever speeds they found natural. (*B*) Human-preferred walking speeds and model-predicted optimal walking speeds. Humans walk slower for smaller radii, as also predicted by energy optimality. The yellow box plot shows human preferred walking speed along with individual data points (box indicates 25$^{\mathrm{th}}$ percentile, median, and 75$^{\mathrm{th}}$ percentile, and whiskers indicate the range). The solid dark blue line is the optimal tangential speed v_{opt} for every radius. Also shown are two bands denoting speeds, for which the metabolic cost per distance is within 1% (lighter blue) and 2% (darker blue) of the optimum cost. Most humans seem to be within 2% of their energy optima. Sensitivity of these predictions to uncertainty in the metabolic model coefficients is shown in *SI Appendix*, Fig. S2. (*C*) Metabolic cost per unit distance per unit mass. Minimizing this function at each radius produces model predictions in *B*, identical to the dark blue line in *C*. (*D*) The turning cost per unit distance is linear in velocity ($\alpha_3 v/R$) and modifies the walking cost in a manner that the optimal speed is lower for smaller radii or higher curvatures. (*E*) The optimal metabolic cost per unit distance as a function of the radius.

An Outline: Energy-Optimal Behavioral Predictions vs. Experiment. In the rest of this section, we alternate between making behavioral predictions from energy optimization and comparing these predictions with experiment. First, we consider simple tasks such as walking in circles, turning in place, and walking in straight lines: tasks in which the movement path is fixed. For these tasks, we directly use the metabolic model in Eq. **1**. Then, we consider more complex tasks that require the movement paths to be selected by the subject: for these tasks, we first generalize the metabolic energy model in Eq. **1** by incorporating other prior metabolic data (as in Eq. **2**, presented later), thereby accommodating more general locomotion and arbitrary paths.

Prediction: Optimal Speeds Are Lower for Smaller Circles. When walking a long-enough distance in a straight line in the absence of time constraints, humans usually walk close to the speed that minimizes the total metabolic cost per unit distance $E' = \dot{E}/v$ (2, 4, 5, 23). This energy-optimal speed is sometimes called the maximum range speed (23), as it also maximizes the straight-line distance traveled with a fixed energy budget. Analogously, for walking in circles (Fig. 2*A*), we hypothesize that humans will use speeds that minimize the total cost per unit distance $E' = \dot{E}/v = \alpha_0/v + (\alpha_1 + \alpha_2/R^2)v$. This cost per unit distance is minimized when the slope $\partial E'/\partial v = 0$—that is, at the speed $v_{\text{opt}} = \sqrt{\alpha_0/(\alpha_1 + \alpha_2/R^2)}$ (Fig. 2*B*). This optimal speed v_{opt} is lower for lower radius R, thus predicting that humans would prefer to walk slower in smaller circles (Fig. 2*B*). Fig. 2 *C* and *D* provide intuition for how the turning cost lowers the optimal speed for circle-walking. The quantity minimized here, namely, the mass-normalized cost per unit distance E', is a scaled version of the cost of transport (10, 23), a nondimensional quantity given by E'/g.

Experiment: Human Preferred Speeds Are Lower in Smaller Circles, as Predicted by Energy Optimality. We asked people to walk naturally on circular paths of four different radii and in a straight line (Fig. 2*A*). As predicted by energy optimality, we found that humans preferred lower speeds for smaller circles (Fig. 2*B*; ref. 24). The median preferred speed across subjects was well predicted by the energy-optimal speed at every radius, and essentially all of the preferred speeds at any radius were within 2% of optimal energy cost (Fig. 2*B*). In this walking-in-circles experiment, humans were clearly able to walk at faster or slower speeds than optimal at each radius, as demonstrated in our earlier metabolic trials (Fig. 1). For the special case of straight-line walking, the optimal speed is given by $v_{\text{opt}} = \sqrt{\alpha_0/\alpha_1} = 1.35$ m/s, which agrees with typical human preferred walking speeds in previous studies (5, 23, 25), as well as the trials here. Further, for every single subject and every single trial, the data were such that their average preferred speed for a larger-radius circle was higher than that of a smaller circle ($v_{\text{pref,4m}} > v_{\text{pref,3m}} > v_{\text{pref,2m}} > v_{\text{pref,1m}}$).

Corollary: A Straight-Line Path Is Optimal If There Are No Other Constraints or Obstacles. Conventional wisdom dictates that (in the absence of other constraints), a straight-line path would be energy-optimal to travel a given distance between two points A and B. This conventional wisdom relies on implicit assumptions about the metabolic energy landscape unavailable before our measurements. Assume that the distance to be traveled is long enough (5) so that we minimize the metabolic cost per unit distance $E' = \dot{E}/v = \alpha_0/v + (\alpha_1 + \alpha_2/R^2)v$, ignoring any small initial or final transient costs. Then, at any speed, this cost is minimized when the turning radius R goes to infinity. This result is reflected in Fig. 2*E*, which shows the minimum cost per unit distance at any given turning radius, and the minimum is achieved when radius R goes to infinity. Because the straight line both minimizes the distance traveled and the cost per unit distance, the straight line minimizes the total cost for a given distance. Such optimality of straight-line walking will be true for any metabolic-rate model that has positive cost penalty for turning, not necessarily the specific functional form we have considered here. However, as noted earlier, we considered functional forms for the metabolic cost that allowed turning to result in energy reduction—e.g., negative α_2 or a linear term in $|\omega|$ with a negative coefficient. Such metabolic-cost functions were not justified by our metabolic data (*SI Appendix*, Table S1). Of course, the optimality of the straight-line path is not generally true in the presence of obstacles or constraints such as those on initial and final body orientation, as consider later in this section.

Prediction: Minimizing Energy Cost of Turning in Place Predicts an Optimal Turning Rate. Humans often need to turn in place while standing, to reorient their body—to face a new direction. Turning in place or spinning in place (Fig. 3*A*) is a special case of walking in circles with radius $R \to 0$ and speed $v \to 0$, while the angular velocity $\omega = v/R$ remains nonzero. Extrapolating using these limits, we obtain the metabolic rate of turning in place to be: $\dot{E} = \alpha_0 + \alpha_2\omega^2$. The metabolic cost of turning in place per unit angle (analogous to metabolic cost per unit distance) is $\dot{E}/\omega = \alpha_0/\omega + \alpha_2\omega$. This cost per unit angle is optimized by steady optimal turning speed $\omega_{\text{opt}} = \sqrt{\alpha_0/\alpha_2} = 1.46$ rad/s = 83.6 degrees/s (Fig. 3 *B* and *C*).

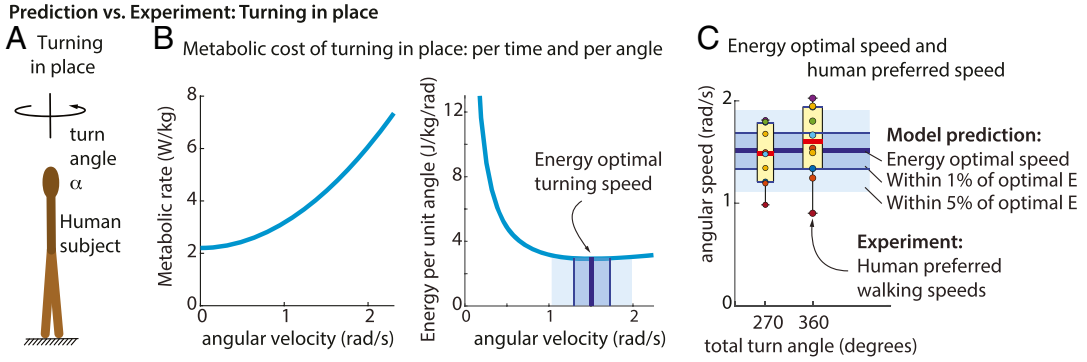

Fig. 3. Prediction vs. behavior: turning in place. (*A*) To further test behavioral predictions of energy optimality, we asked subjects to turn by a given angle α, starting and ending at rest. (*B*) Metabolic rate and the cost per unit turning angle, obtained by extrapolating the model to turning in place. The blue lines and bands shown denote optimal turning speeds and the set of speeds within 1% or 5% of optimal energy cost. (*C*) Human preferred turning speeds (yellow box plot and individual data points) largely overlap with the turning speeds within 5% of the optimal cost. Sensitivity of these predictions to uncertainty in the metabolic model coefficients is shown in *SI Appendix*, Fig. S2.

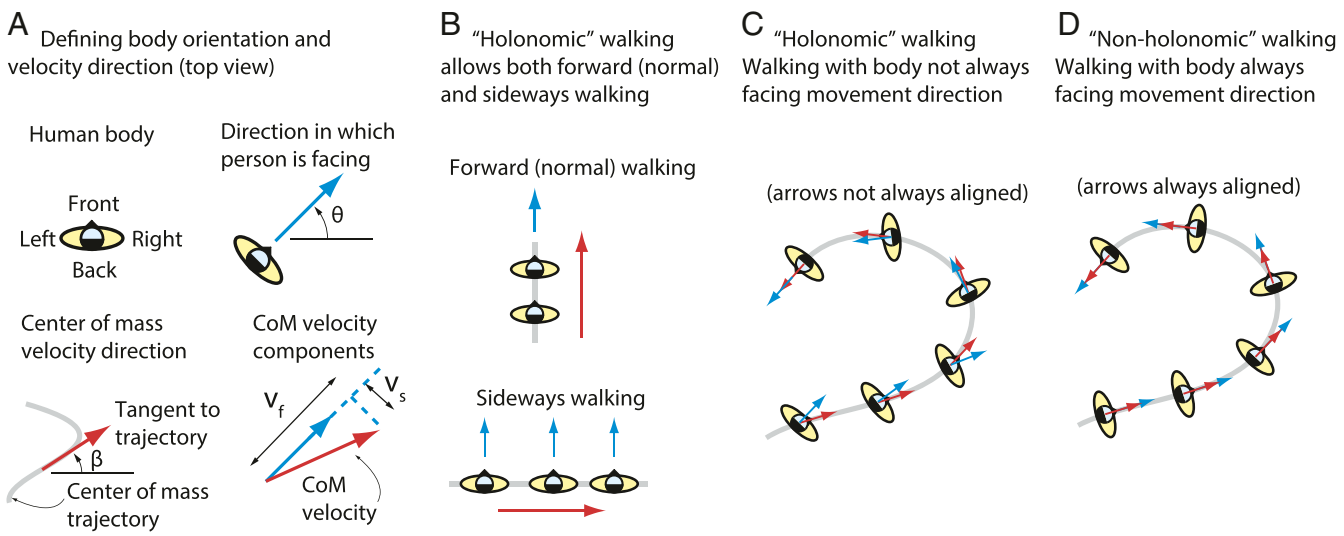

Fig. 4. Two kinds of walking: face where you are going or not. (*A*) Visual representation of the body from a top view, introducing different notations for the direction in which the body center of mass (CoM) is moving (red arrow) and the body orientation (blue arrow). The components of the center-of-mass velocity are shown to be v_f and v_s in the anteroposterior (forward) and medio-lateral (sideways) directions, respectively. (*B*) While forward walking has body orientation aligned with movement direction, it is possible to walk sideways, so that the body orientation is perpendicular to the movement direction. (*C*) Walking in a manner that the body orientation need not be aligned with the movement direction (holonomic)—that is, the blue and red arrows need not be aligned. (*D*) Walking in a manner that the body orientation is the same as the movement direction (nonholonomic)—that is, the blue and red arrows are aligned.

Experiment: Humans Turn in Place at Close to the Energy-Optimal Turning Rate. We performed behavioral experiments in which humans turned in place by a fixed turn angle α (Fig. 3*A*), starting and ending at rest. The average human turning speeds for large turns of 270° and 360° largely overlapped with each other and almost entirely overlapped with the set of steady turning speeds that were within 5% of the optimal turning cost (Fig. 3*C*).

Two Ways of Generalizing to Complex Paths: Face the Movement Direction or Not. We now generalize the metabolic cost of walking in circles to walking on arbitrary paths, but, first, we discuss what assumptions such generalizations make. When walking, we can conceptually distinguish between the direction in which our body moves (velocity direction, angle β; Fig. 4*A*) and the direction in which the body faces (body torso orientation, angle θ). For instance, in normal straight-line walking, these two directions are aligned ($\theta = \beta$), but in "sideways walking" (6), the body moves perpendicular to how the body faces (Fig. 4*B*). Thus, it is not essential that we walk in a manner that we always face the movement direction. So, we consider two ways of walking: walking while not always facing the movement direction (Fig. 4*C*) and walking while always facing the movement direction (Fig. 4*D*). We call these kinds of walking "holonomic" and "nonholonomic ," respectively, borrowing this terminology from classical mechanics, control theory, and other prior work on locomotor paths (17, 26, 27). The term nonholonomic simply implies that the system obeys a velocity constraint—here, the constraint is that the body velocity direction is always along body orientation. Holonomic walking has no such velocity constraint, and, thus, nonholonomic walking is a special case of holonomic walking. We generalize the metabolic-cost model of Eq. **1** to both these types of walking (17). Specifically, for holonomic walking, in which the body need not face the movement direction, we use the following revised metabolic cost of the form:

$$\dot{E} = \alpha_0 + \alpha_1 v_b^2 + \alpha_2 \omega^2 + \alpha_s v_s^2, \qquad [2]$$

where v_b is the body velocity component in the forward or anteroposterior direction (in the direction that the body is facing) and v_s is the body velocity component in the sideways or medio-lateral direction (perpendicular to how the body is facing) (Fig. 4*A*). Here, we refer to Eq. **2** along with an additive cost for changing speeds (5) as the "generalized metabolic-cost model." See *Materials and Methods* for further details. The rest of this article uses this generalized cost model to make predictions about how people walk in more complex situations involving turning. Because holonomic walking is more general, we use this type of walking to make predictions in the rest of this main manuscript, but we also show results from nonholonomic walking in *SI Appendix*, Fig. S3.

Prediction vs. Experiment: Navigating from A to B with Constraints on Initial and Final Direction. Mombaur et al. (17) performed human-subject trials in which the human started from rest at point A and ended at rest at point B, starting and ending with different body orientations (Fig. 5*A*). The required body orientations were provided as arrows drawn on the ground. Subjects were not constrained in any other way, say, by obstacles or time limits. Having different required body orientations at A and B required the subjects to turn. For seven different end-point and body-orientation combinations, we computed the metabolically optimal turning trajectory with our model and using trajectory optimization (*Materials and Methods* and *SI Appendix*). We performed two versions of the calculation, one holonomic and the other nonholonomic. Remarkably, we found that the holonomic model—that is, allowing body orientation to be different from movement direction—predicted the time progression of body position (x vs. t and y vs. t) and body orientation (θ vs. t) without fitting to these behavioral data (Fig. 5 *B–D*). In both the predicted optimal paths and the human paths, the body orientation was not always aligned with movement direction. Constraining body orientation to be aligned with movement (nonholonomic walking) produced worse predictions of body position and orientation (*SI Appendix*, Fig. S3; see also ref. 17).

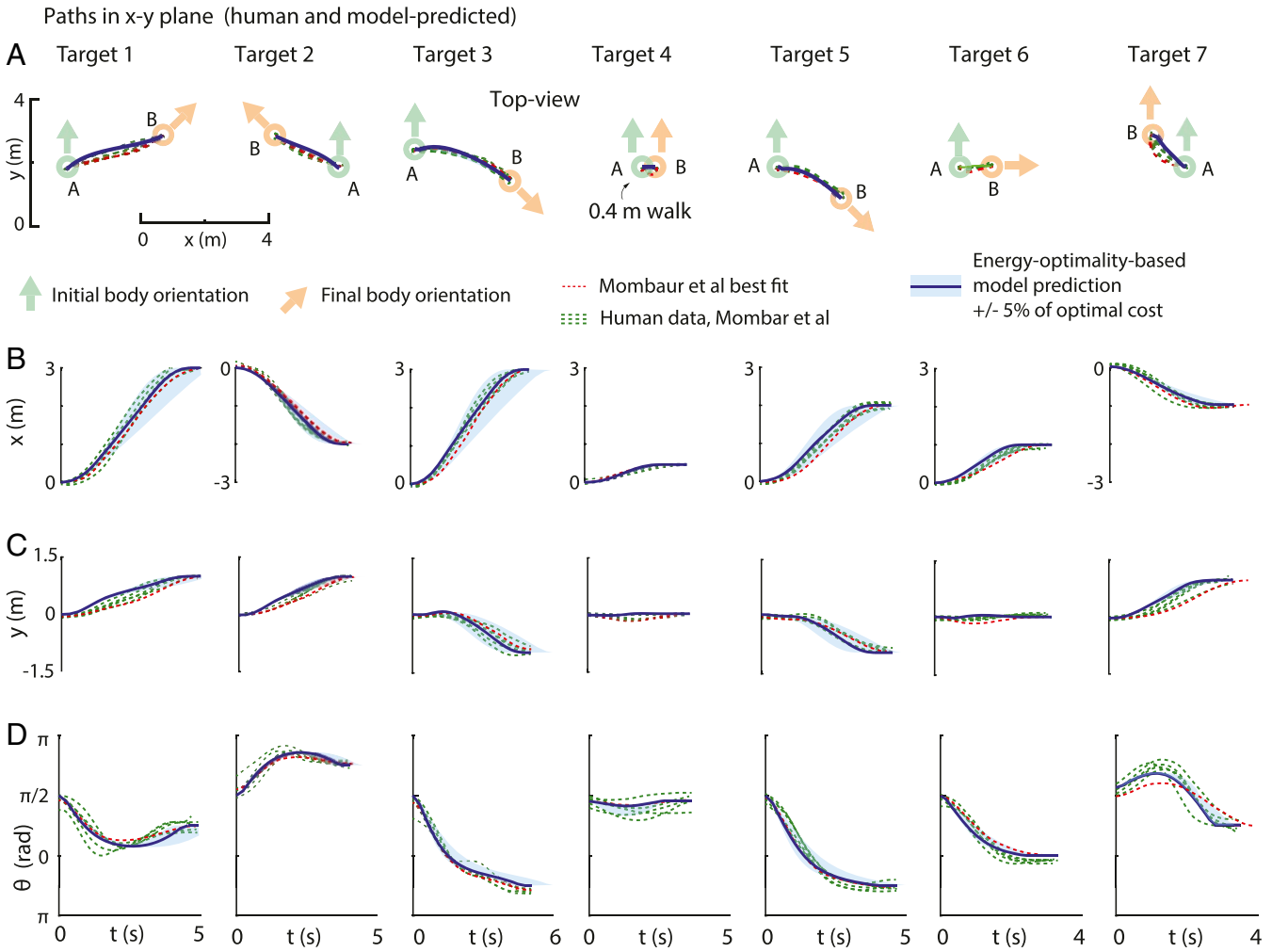

Fig. 5. Prediction vs. behavior: path planning, starting, and ending at rest. (*A*) Mombaur et al. (17) asked subjects to walk short distances, starting at rest at point A and ending at rest at point B. The subjects had to start facing one direction (light green arrow) and end facing possibly another direction (orange arrow). (*B–D*) The body position (x, y) and body orientation θ as a function of time. Holonomic model predictions are solid dark blue, with a light blue band indicating trajectories withing 5% of the optimum cost; experimental data are dashed dark green, and the best-fit model in Mombaur et al. (17) is indicated as a dashed red line. We see that our energy-optimization-based model predictions mostly pass through the center of the experimental data. Just for targets 3 and 7, subjects started and ended with slightly different body orientations than prescribed, so these were used in the optimizations presented. See *SI Appendix*, Figs. S1 and S2 for variants of this figure with alternate assumptions. Task 4 involved the most striking difference between these holonomic model predictions vs. the nonholonomic model predictions (*SI Appendix*, Fig. S1); this task required simply moving sideways by a short distance.

Prediction vs. Experiment: Navigation around and between Two Doorways. In another set of previous studies (18, 26, 28), researchers instructed human subjects to walk through two sets of doors, A and B, facing in different directions and separated by a few meters (Fig. 6*A*). The subjects started from rest 2 m before A and ended 2 m beyond B. As in ref. 17, humans chose smooth paths that gradually turned, rather than, say, achieving the same task using sharp turns or too many direction changes (Fig. 6 *B* and *C*). Again, we used trajectory optimization to compute the energy-optimal way of performing this task. The resulting optimal trajectories are similar to the human trajectories in data (Fig. 6), which are within 2% of the optimal cost (*SI Appendix*, Fig. S3). The predictions from the holonomic and nonholonomic models are almost the same, with the nonholonomic model taking a slightly wider turn near the door. For these longer-distance bouts (compared to those in Fig. 5), even when the walker is not constrained to be nonholonomic, it is energy-optimal to be nearly nonholonomic—that is, walk in a manner that the body nearly faces movement direction, as also observed in experiment (26). *SI Appendix*, Fig. S6 shows how the body movement direction β closely follows body orientation θ. The difference between the two angles ($\beta - \theta$) reduces as the distance traveled increases.

An important constraint for the optimal path calculation here, in contrast to those for Fig. 5, is that the body path does not intersect with the doors and has a minimum clearance from the doors. The clearance used is consistent with typical human dimensions (29) and also with behavioral data (16). In the absence of such a clearance constraint, the optimal path ignores the walls of the doors and shows a sharper turn near the end-point B. Thus, explaining human behavior may require considering constraints such as avoiding obstacles (here, the doorways), in addition to minimizing energy-like cost functions.

Corollary: Shortest Paths Are Not Optimal and Not Used by Humans. In the previous two tasks (Figs. 5 and 6), our model predicted gradually turning paths as also exhibited by the human subjects.

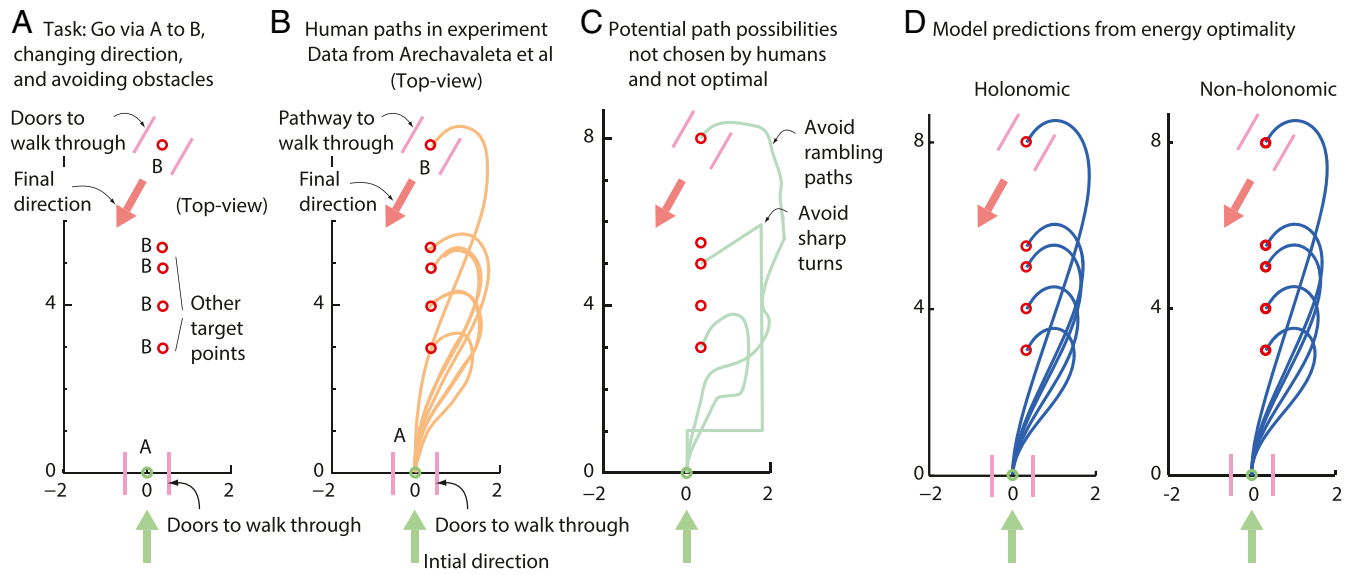

Fig. 6. Prediction vs. behavior: navigating around and through doors. (*A*) Humans were asked (19) to walk through a doorway at point A (pink parallel lines) to another doorway at point B, stopping 2 m beyond the second door. The second door B had five different locations, as shown (red circles). The walls of the doorways serve as obstacles to be avoided. (*B*) Human data redrawn from ref. 19 are for head paths. (*C*) A human or the model is capable of sharp turns and otherwise complex paths to achieve the task. But model predictions for the body path from energy optimality are qualitatively similar to human paths, despite not having to constrain the average velocity as in ref. 19. See *SI Appendix*, Fig. S5 for bands containing trajectories within 2% of the optimal cost.

These paths are not the shortest paths between the origin and destination: the shortest paths for the tasks in Fig. 5 are straight lines, whereas those for the tasks in Fig. 6 are straight-line paths interspersed by a circular arc around a door. Thus, humans walk for a longer distance than necessary to save energy, even on flat terrain. This nonoptimality of the shortest path is due to the additional cost for turning, without which the shortest path would be energy-optimal.

Prediction vs. Experiment: Humans Slow Down Turning a Corner while Navigating an Angled Corridor. A common everyday task is turning a corner in an angled corridor (Fig. 7*A*). A previous study by Dias et al. (16) had subjects walk around angled corridors and measured the walking speeds during the turn. Again, using trajectory optimization, we computed the metabolically optimal path in such angled corridors, specifically computing the walking speed during the turn. We found that the optimal walking speed was lower during the turn and that this turning speed was lower for greater turn angles (Fig. 7 *B* and *C*). Further, the experimentally observed human speeds from ref. 16 were almost identical to the model-predicted turning speed; the distribution of human turning speeds overlapped with the model-predicted band of speeds within 2% of the optimal cost (Fig. 7*C*). Speed reductions during turns were similarly

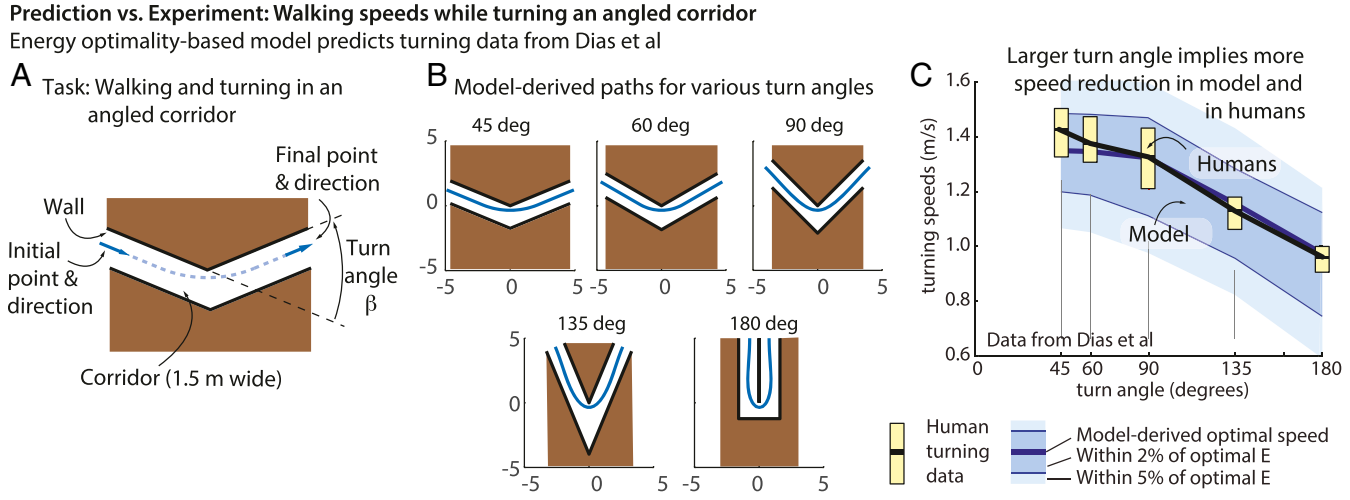

Fig. 7. Prediction vs. behavior: navigating an angled corridor. (*A*) A turning task, involving walking along a straight corridor and turning into another corridor angled with respect to the first. (*B*) Energy-optimal paths for the task. Subject enters the first corridor and leaves the second corridor in a straight-line path at their energy-optimal speed and clears the wall. (*C*) Experimental data from Dias et al. (16) (mean ± SD) show that the human speeds during the turn are lower for larger turn angles, as also predicted by the model-derived energy-optimal paths. The human speed distribution is entirely contained within the set of speeds within 2% of the optimal cost.

observed by Sreenivasa et al. (30), who considered turning in a cyclical task that alternated between turning and straight-line walking. In all these turning tasks, as predicted by the model, humans do not usually use sharp turns when smooth turns are possible.

Rectilinear Walking Speeds Are Predicted as a Special Case. The optimality criterion proposed here predicts rectilinear or straight-line walking phenomena as a special case. Specifically, it predicts that typical steady human walking speeds should be around $v_{\text{opt}} = \sqrt{\alpha_0/\alpha_1} = 1.35$ m/s, which agrees with preferred walking speeds over longer distances in previous studies (5, 23, 25). Seethapathi and Srinivasan (5) used a straight-line walking metabolic model along with a cost for changing speeds to predict lowered walking speeds for short-distance bouts. Our generalized metabolic-cost model contains the model of ref. 5 as a special case (by construction) and, thus, also predicts that humans should walk systematically slower for shorter distances. Similarly, Handford and Srinivasan (6) showed that when asked to walk sideways, humans walk close to the energy-optimal sideways walking speed (about 0.6 m/s). Again, the generalized holonomic model contains the sideways walking model of ref. 6 as a special case (by construction) and makes similarly low-speed predictions for sideways walking.

Prediction vs. Experiment: To Go Sideways, Walk Sideways or Turn and Walk Forward. Humans do not usually walk sideways. Handford and Srinivasan (6) showed that sideways walking costs three times more energy than walking forward at their respective optimal speeds. Now, consider a situation in which someone wants to go from A to B, but is initially (and finally) facing perpendicular to the line AB (*SI Appendix*, Fig. S7). That is, they want to move sideways—e.g., they are working at a kitchen counter and want to move sideways. Should they walk sideways or turn by 90° and walk facing forward? To make a prediction, we compared the cost of walking sideways and the cost of turning and walking forward and turning again. This comparison predicted that humans should walk sideways for distances less than 0.8 m; for larger distances, walking sideways is more expensive than turning and walking facing forward. Indeed, target 4 in Fig. 5 asks subjects to travel sideways by 0.4 m, starting and ending facing forward (17). Subjects, as predicted, did not turn and walk forward; instead, they just stepped sideways while mostly facing forward.

The Predictive Power of Minimizing Metabolic Energy vs. Other Optimality Hypotheses. We have predicted a wide variety of experimentally measured human locomotor behavior, with no fitting to these behavioral data, by directly minimizing an empirically based metabolic model of walking. We now briefly compare the energy-cost-based hypothesis with some other hypotheses that have been explored. Smooth body trajectories can be predicted by cost functions that maximize smoothness, such as acceleration, "jerk" (derivative of acceleration), or "snap" (second derivative of acceleration). Such cost functions have been successful in arm reaching (31), but they have also been employed to predict walking trajectories (17, 18). However, such smoothness-maximizing cost functions, taken seriously, produce two unecological predictions. First, they cannot predict the velocity at which people move: specifically, the optimal way to minimize jerk or snap is to perform a task with infinitesimal speed over an arbitrarily long period. See *SI Appendix*, section S4 for a mathematical account of using these smoothness objectives. Thus, such smoothness-maximizing cost functions require a constraint on the average velocity of the task to produce meaningful results. In contrast, our metabolic-energy approach naturally produces an optimal velocity for any task, without having to constrain it. A second consequence of the jerk-minimization hypothesis, even with a velocity constraint, is that it produces "scale-invariant solutions." That is, for the tasks in Fig. 6*A*, it produces paths that "look the same" for a 10-m walk vs. a 10-km walk, producing many-kilometer-long path excursions that humans would never use.

Arechavaleta et al. (19) used an objective function equal to the integral of $(v^2 + \dot{\kappa}^2)$ over the path, where $\dot{\kappa}$ is the rate of change of path curvature. Again, minimizing this objective without a further constraint predicts that humans should move at infinitesimal velocity. So, in their calculations, Arechavaleta et al. (19) constrained the total time. Thus, these minimization hypotheses require further assumptions about human behavior, which need not be made with the more parsimonious energetics-based approach.

Finally, Mombaur et al. (17) used a model-fitting procedure to select an objective function that best predicts human walking trajectories in their experiments. Their objective function had terms related to linear and angular velocity acceleration, work, jerk, and task time duration. However, their best-fit cost function, because it is dominated by linear and angular acceleration terms, cannot explain observed speeds for walking in circles, turning in place, or walking in a straight line for longer distances. Thus, each of these previous cost functions could be considered as overfit to one or two experimental conditions and cannot predict all of the diverse phenomena predicted by our model. On the other hand, the true objective may well contain terms analogous to those used in these prior works (17–19), in addition to those in our metabolic model; for instance, smoothness-promoting terms related to acceleration or jerk, as a proxy for costs related to muscle forces and force rates (32–34). Such terms may be useful in explaining smoother speed changes (better than our model can) when speed changes are needed, for instance, during gait initiation and termination (35).

Discussion

We have provided a unified theoretical account of human navigation paths and speeds. We first measured the energetics of humans walking with turning and showed that the energy cost has a substantial dependence on path curvature. Turning increased the locomotor cost, and this turning cost increased with the turning speed. We then used the experimentally derived metabolic-energy model to predict energy-optimal walking behavior in various contexts, explaining many disparate experimentally measured and ecological human locomotor behavior, some via additional experiments that we performed and some by comparison with data from prior experimental studies on human navigation. Importantly, our theoretical account also makes predictions about straight-line locomotion as special cases, predicting steady walking speeds and short distance speeds when turning is not required. Thus, we have presented a unified theoretical account of both straight-line and more general curvilinear human walking.

We showed that the tendency to slow down when turning and slow down more when turning in a smaller radius can be explained by energy optimality. One alternate hypothesis for slowing down while turning is to avoid slipping. While fast-moving cars and bicycles slow down on curves to avoid slipping, humans in our experiments were far from any danger of slipping. We estimated the foot–ground friction coefficient as $\mu = 0.6$ to 1.2, giving friction cone angles of 30° to 50° ($= \tan^{-1}\mu$). But the maximum leg angle in our circle walking (1 m at 1.5 m/s) was 12°, much less than the friction cone angles, giving a large safety factor from slipping.

The speed reductions found here due to path curvature are reminiscent of speed reductions when humans try to run as fast as possible around a circle (36, 37). However, these tasks are different in one important respect: while our subjects are able to walk faster or slower compared to their preferred speeds,

maximal-speed running does not have this property (by definition). Nevertheless, there may be mechanistic similarities between the two cases. As was initially thought for maximal running (36, 37), we might hypothesize that the increased walking metabolic cost may be due to the necessity for producing a centripetal force; see refs. 33, 34, and 38–41 for accounts of force costs in locomotion. However, using elementary formulas for centripetal accelerations (36), we estimated that for the fastest walking speed at the smallest radius, the leg-force requirements increased only by 1.3% (*SI Appendix*, section S3). This small force increase cannot directly account for the nearly 50% increases in metabolic costs we have measured. Similarly, if we conceptualize the additional centripetal acceleration as increasing the "effective gravity" (resulting in the increased leg forces) by 1 to 2%, then the leg-work requirements would also increase by a similar small percentage, and not by over 50% (12, 42, 43). One might speculate that the larger increases in metabolic rate may be partly due to recruitment of additional muscles that may not be at their optimal operating regimes (37).

The cost of turning could also be due to the work necessary to turn the body orientation, given that the body has a nonzero rotational inertia (44). Per our assumed metabolic-cost-model form, the metabolic cost of turning in place was $\dot{E} = \alpha_0 + \alpha_2\omega^2$. Turning in place only requires body-orientation changes and does not require centripetal forces. Thus, this cost model for turning in place is consistent with the premise that most of the increased cost due to turning (namely, $\alpha_2\omega^2$) is to accomplish body-orientation changes (*SI Appendix*, section S3). The increased metabolic cost could potentially be understood by measuring the body movements and the ground-reaction forces (24, 45, 46), performing inverse dynamics (15) and examining which joints have greater torques or perform more work.

Our metabolic-cost model is empirical in nature, so that to generalize it to different situations (e.g., running or uneven terrain), we may need to repeat the metabolic experiments for that new situation. An alternate path to potential generalization is via a three-dimensional (3D) dynamical model of a biped (47, 48), first showing that it is able to predict the walking metabolic measurements here (and, along the way, also incorporating the stepping dynamics, ignored here for parsimony). But, such 3D biped models may still not generalize to other human populations—for instance, those with movement disorders, whether due to musculoskeletal or neurological differences, because predictive understanding of movement behavior with movement disorders without task- or population-specific fitting is largely open. On a related note, we have assumed left–right symmetry in fitting the metabolic-cost model (Eq. **1**), but bodily asymmetries may translate to energetic asymmetries in turning, e.g., in unilateral amputee populations. Accounting for such asymmetries in the metabolic model, one can then examine whether no turning ($\omega = 0$) still minimizes the metabolic rate for speed v and whether a straight-line path remains energy-optimal.

One could conjecture that there are greater stability issues while turning and that these stability issues contribute to the subjects being cautious and lowering their speed. However, such conjecture seems unnecessary, as energy minimization seems to largely explain the speed reductions. An open question in movement control is to what extent humans prioritize energy or effort on the one hand and stability or robustness to uncertainty on the other (49). This question is beyond the scope of this study, as we have based our behavioral predictions on empirically derived energy costs. The experimentally measured energy costs already include any trade-offs that humans had to make to walk efficiently and stably (50, 51). Thus, we should distinguish our empirical optimality criterion from the theoretical limit of true energy optimality, requiring perfect control and the absence of perturbations or uncertainty.

In the real world, there may be other, additional concerns that may make a human walk faster than energy-optimal—for instance, a cost for time or constraints on time taken to complete the movement (4, 52). Here, we have considered conditions where no such explicit time pressure exists. Deviations from deterministic energy optimality may also be due to optimality in a Bayesian or probabilistic sense (53) in the presence of uncertainly or due to interactions with or navigating around another moving human.

It is sometimes argued that energy optimality or energy economy may be useful only in "steady-state tasks," as opposed to "transient tasks," or may only be useful when the energy saved is substantial (5). Here, we have shown broad agreement of behavior with empirical energy optimality in short transient tasks (e.g., the turning part of a corner) that consume a very small amount of energy. For instance, we estimate the total energy cost of a turn in the angled corridor (Fig. 7) to be about 10 J/kg. So, the savings relative to a nonoptimal turn (e.g., not slowing down or using a sharper turn) are a small fraction of this cost, equivalent to just over a second of resting-energy expenditure. Here, as in many of the situations we considered, the experimentally observed behavior was within 2% of the optimal energy costs from the model, corresponding to similarly small amounts of energy differences (0.2 J/kg, equivalent to resting-energy expenditure for one-seventh of a second). That energy optimality provides an account of diverse transient behavior with low energy requirements is perhaps an indication of how much the nervous system values energy savings, all else being equal. Our results are agnostic to how the near-energy optimality is achieved, whether it is hard-wired evolutionarily, acquired while learning to walk during childhood, or the energy-optimal trajectories are computed in real time by the nervous system (54, 55). It is likely a mixture of all such mechanisms: energy optimality correctly predicted lowered walking speeds for shorter distances [a task with low total energy (5)], walking speeds in sideways walking [an uncommon task (6)], and stride frequency in the presence of an external exoskeleton [an uncommon task with dynamic changes in the energy landscape (7, 54)].

The neural mechanisms underlying such energy optimality or locomotor navigation are yet to be elucidated (56). Further, the aspects of navigation we focused on were path and speed selection, when all information about the world is fully available, and we did not consider aspects involving sensing, information gathering, and course correction, or topological aspects in which one among multiple (potentially locally optimal) paths around obstacles need to be selected (57, 58).

Our results suggest further behavioral experiments to test model predictions and inform improvements to the model: for instance, walking through via points with freedom to choose the intervening path, comparing walking sideways vs. turning, walking around obstacles, walking around moving obstacles (such as other people), etc. We obtained a cost of spinning in place by extrapolation, whose accuracy can be improved by using smaller radii. Because of this extrapolation, we would a priori expect the current model to be less reliable in tasks that require sharp direction changes. Mechanisms for the turning cost could be probed by predicting and testing experimentally how the cost varies after various manipulations of the system: adding mass or moment of inertia to the trunk or the legs (44) or providing centripetal forces via a tether, as in ref. 37. Our empirical metabolic-cost model could be tested further by energetic measurements of humans walking on sinusoidal paths, achieved by moving side to side on treadmills. Such curvilinear paths with nonconstant curvature may allow us to disambiguate energy-cost dependence on v and ω vs. their derivatives, which may be more significant for more unsteady tasks.

The metabolic model for curvilinear locomotion presented here may help improve the estimates of daily metabolic expenditure obtained by, say, using wearable devices. Studies have found that about 20% of steps in household settings (59) and 35 to 45% of steps in common walking tasks in home and office environments involve turns (1), so neglecting the cost of turning may result in erroneous estimates of energy expenditure. Further ambulatory studies tracking people over many days with wearable sensors (60) could help to estimate the magnitude of this error.

As noted earlier, reduced maximal running speeds around a circle have been measured (36, 37), but submaximal running studies measuring metabolic costs have not been performed. Generalizing our metabolic model to running may better help estimate the metabolic cost during sports (e.g., soccer), which involve extensive speed and direction changes. Understanding human locomotion while turning would also be a useful tool in rehabilitation or assistive robotics. Robotic legs, prostheses, and assistive devices are often designed with an emphasis on straight-line walking. So, better understanding turning mechanics (for instance, by providing targets of turning performance) may inform designing for real-world scenarios where curvilinear locomotion is essential.

In conclusion, through experiments and mathematical models, we have provided a unified theoretical predictive account of human walking in non-straight-line paths and with turning from the perspective of energy optimality. We have suggested further experiments to test model predictions, to inform model improvements, and to generalize the models to other populations and other tasks.

Materials and Methods

We performed three different experimental studies, one for measuring the metabolic cost of turning and two for measuring human behavior while turning. We performed multiple model-based optimization calculations to predict energy-optimal trajectories and speeds under different task constraints to compare with a number of different behavioral experiments, including our own.

Experiment: Metabolic Cost of Humans Walking in Circles. All experiments were approved by The Ohio State University's Institutional Review Board, and all subjects participated with informed consent. Subjects were instructed to walk along circles drawn on the ground (Fig. 1*A*). The subjects were instructed to keep the circle directly beneath their feet or between their two feet, but not entirely to one side of their feet. All subjects walked with the circle between their feet with nonzero step width. We used four different circle radii ($R = 1, 2, 3, 4$ m, $N_{\text{radii}} = 4$). At each radius, subjects performed four walking trials, each with a different constant tangential speed v in the range 0.8 to 1.58 m/s, resulting in $N_{\text{trials}} = 16$ trials per subject; one subject performed fewer trials ($N_{\text{trials}} = 13$). Tangential speeds were prescribed by specifying a duration for each lap around the circle. A timer provided auditory feedback at the end of every half-lap duration (for $R = 3, 4$ m) or full-lap duration (for $R = 1, 2$ m), so that subjects could speed up or slow down as necessary. Within a few laps of such auditory-feedback-driven training, subjects walked at the desired average speed, completing each lap almost coincident with the desired lap time. Subjects maintained the speed with continued auditory feedback for 6 to 7 min: 4 min for achieving biomechanical and metabolic steady state and 2 to 3 min for computing an average metabolic rate $\dot{E}$. Subjects used clockwise or counterclockwise circles as preferred. Subjects were instructed to walk and never jog or run; all subjects always walked. Overall, this resulted in nearly 35 h of subjects walking in circles.

The trial order was randomized over speed and radius for seven subjects (mass 77.3 ± 10 kg, height 1.79 ± 0.05 m, mean $\pm$ SD, and age range 22 to 27), whose data are presented in detail in *Results*. For 10 other subjects (mass 73 ± 14 kg, height 1.75 ± 0.13, mean $\pm$ SD, and age range 21 to 27), the trial order increased monotonically in speed and radius. The overall regression relations were similar when both sets of data were analyzed in the same manner, suggesting no large order effect. Metabolic rate per unit mass $\dot{E}$ was estimated during resting and circular walking by using respiratory gas analysis (Oxycon Mobile with wind shield, < 1 kg): $\dot{E} = 16.58\,\dot{V}_{O_2} + 4.51\dot{V}_{CO_2}$ W/kg with volume rates $\dot{V}$ in mL·s^{-1}·kg^{-1} (20). Subjects exhibited small, but systematic, differences between prescribed lap times and lap times estimated from video. So, in subsequent analyses, we used corrected values for v and ω by using the estimated lap times in their calculation (speed = circumference/lap time, angular speed = 2π/lap time). See Dataset S1 for the collected data, including these corrections. To improve estimates of the steady-state metabolic rate and to test if the transients had subsided, we fit an exponential to the last 3 min of metabolic data and determined the extrapolated steady state (61, 62). This extrapolation resulted in less than 2% changes in any of the coefficients in Eq. **1**, compared to the standard procedure of using the mean metabolic rate over the last 2 or 3 min. This comparison suggests that the standard procedure suffices. Reported significance of metabolic differences across radii were tested via one-sided t tests with a Bonferroni correction for multiple comparisons. Linear regressions used fitlm in MATLAB.

Experiment: Preferred Walking Speeds in Circles. Subjects' preferred walking speeds were measured by asking them to walk in a straight line and along circles (24) of radii (R) equal to 1 m, 2 m, 3 m, and 4 m at whatever speed they found comfortable (Fig. 2*A*); the subjects walked for about 100 m in each of these trials (four 4-m laps, eight 2-m laps, etc.). The subjects were told beforehand how many laps they would need to complete and were asked to do whatever felt normal or natural. We measured the time duration T for the second half of the walk from video and estimated the average tangential speed as the distance traveled around the circle divided by the time duration; that is, the average tangential speed was $(2\pi R \cdot n_{\text{laps}})/T$, where n_{laps} is the number of laps considered. Two trials were performed for each radius, and all trials were in random order of radii. The subject population for these trials (mass 73.6 ± 10 kg, height 1.74 ± 0.13 m, age 22.6 ± 1.7 y, and 90 trials with $N = 9$) was distinct from those in the previous experiment.

Experiment: Preferred Turning-in-Place Speeds. Subjects' (mass 73.4 ± 11 kg, height 1.75 ± 0.10 m, age 26 ± 5 y, $N = 10$ distinct from earlier samples) preferred turning speeds were measured by asking them to turn in place by 90°, 180°, 270°, and 360° and do whatever felt natural (Fig. 3*A*). Three trials were performed for each turn angle, and the trial orders were randomized. Subjects were free to turn clockwise or counterclockwise in any trial. The average angular velocity of turn was computed by estimating the time taken for turning from video and using the prescribed turn angle. Our goal was to compare preferred turning speeds with model-based predictions of steady-state turning speeds—that is, speeds not affected by the starting and stopping. We found that the average speeds for 270° and 360° turns were similar (Fig. 3), so we infer that these speeds are close to the steady-state speeds. Thus, we used the turning speeds for 270° and 360° turns to test predictions of steady-state turning speeds.

Model: Metabolic Cost of Arbitrary Walking Paths. Our walking-in-circles metabolic experiments constrained the circular paths that the feet travel on rather than the paths that the body travels in. Thus, the radius R and the velocity v in Eq. **1** correspond to the mean trajectory of the feet, rather than the center of mass. If the foot travels in a circle of radius R and has an effective tangential velocity v, the body center of mass travels in a circle of smaller radius R_b and slightly lower tangential velocity v_b. This is because the body leans into the circle, so that the hip is closer to the center of the circle than the foot (36). We first obtained a body-based description of the empirical metabolic cost: $\dot{E} = \alpha_0' + \alpha_1' v_b^2 + \alpha_2' \omega_b^2$, where $\omega_b = \omega = v/R = v_b/R_b$ for circle walking. We find $\alpha_0' = 2.32$ W/kg, $\alpha_1' = 1.28$ W/kg/ $(\text{ms}^{-1})^2$, and $\alpha_2' = 1.02$ W/kg/ $(\text{rad} \cdot \text{s}^{-1})^2$. These coefficients explain the metabolic data roughly as well as the original model (explaining about 88% variance).

Any noncircular or non-straight-line walking path can be described as a curve with constantly changing curvature. That is, each point on the curve has a distinct radius of curvature. If we assume nonholonomic walking, in which the body always faces the movement direction, we can directly apply a metabolic rate of the form $\dot{E} = \alpha_0' + \alpha_1' v^2 + \alpha_2' \omega_b^2$, where v_b is the instantaneous body velocity, $\omega_b = v_b/R_b$ is the body angular velocity, and R_b is the instantaneous radius of curvature. To generalize to holonomic walking—that is, allowing the body to not always face the velocity direction—we distinguished between the body velocity component along the body orientation v_f (forward) and the body velocity component perpendicular to the body orientation v_s (sideways). We then used a metabolic-cost model of the form: $\dot{E} = \alpha_0' + \alpha_1' v_f^2 + \alpha_2' \omega_b^2 + \alpha_s' v_s^2$. This is the same as Eq. **2**. Here, the additional term $\alpha_s' v_s^2$ is the incremental cost of sideways walking (6). Handford and Srinivasan (6) estimated the coefficient α_s' as roughly 7.8 W/kg/$(\text{ms}^{-1})^2$.

Because walking along arbitrary paths may involve or require changing walking speeds, we included the additive metabolic cost of changing speeds, characterized by Seethapathi and Srinivasan (5). This study showed that accounting for this cost predicts lower speeds for short-distance walking bouts using energy optimality, as in humans (5, 35). Eq. **2**, in addition to this work-based cost for changing speeds, is what we refer to as the generalized metabolic-cost model in this manuscript. See *SI Appendix* for more details about the metabolic-cost model.

Model: Energy-Optimality-Based Behavioral Predictions. We compared measured experimental human behavior in a number of different walking tasks to the energy-optimal walking behavior predictions. The energy-optimal walking behavior was obtained by minimizing the total metabolic cost of the walking task. For the simplest two tasks—namely, walking in circle and turning in place (Figs. 2 and 3)—the optimization assumed steady state and required only basic calculus. So, the complete analytical reasoning for the prediction is provided in *Results*. For more complex walking tasks, where the walking path is not predetermined (Figs. 5–7), we solved for the total time duration, body position, body orientation, and their derivatives as functions of time using numerical trajectory-optimization methods (12). For this trajectory optimization, we used the metabolic-cost function described in the previous paragraph. We performed two versions of the optimization, holonomic and nonholonomic, with the latter obeying the constraint that the body always faces the velocity direction. We solved additional optimization problems to obtain trajectories within a certain percent of the optimal cost. See *SI Appendix* for more mathematical details of the numerical optimization.

Data Availability. All study data are included in the article and/or *SI Appendix*.

ACKNOWLEDGMENTS. This work was supported by NSF Grant CMMI-1254842 and its writing in part by an NIH grant R01GM135923-01. We thank Carmen Swain and Blake Holderman for help regarding metabolic equipment during early pilot testing; Alison Sheets for comments on an early draft; and V. Joshi for help with some experimental setups.

1. B. C. Glaister, G. C. Bernatz, G. K. Klute, M. S. Orendurff, Video task analysis of turning during activities of daily living. *Gait Posture* **25**, 289–294 (2007).
2. H. J. Ralston, Energy-speed relation and optimal speed during level walking. *Eur. J. Appl. Physiol.* **17**, 277–283 (1958).
3. J. M. Donelan, R. Kram, A. D. Kuo, Mechanical and metabolic determinants of the preferred step width in human walking. *Proc. Roy. Soc. Lond. B* **268**, 1985–1992 (2001).
4. L. L. Long, M. Srinivasan, Walking, running, and resting under time, distance, and average speed constraints: Optimality of walk-run-rest mixtures. *J. R. Soc. Interface* **10**, 20120980 (2013).
5. N. Seethapathi, M. Srinivasan, The metabolic cost of changing walking speeds is significant, implies lower optimal speeds for shorter distances, and increases daily energy estimates. *Biol. Lett.* **11**, 20150486 (2015).
6. M. L. Handford, M. Srinivasan, Sideways walking: Preferred is slow, slow is optimal, and optimal is expensive. *Biol. Lett.* **10**, 20131006 (2014).
7. J. C. Selinger, J. D. Wong, S. N. Simha, J. M. Donelan, How humans initiate energy optimization and converge on their optimal gaits. *J. Exp. Biol.* **222**, jeb198234 (2019).
8. A. E. Minetti, R. M. N. Alexander, A theory of metabolic costs for bipedal gaits. *J. Theor. Biol.* **186**, 467–476 (1997).
9. A. D. Kuo, A simple model of bipedal walking predicts the preferred speed–step length relationship. *J. Biomech. Eng.* **123**, 264–269 (2001).
10. M. Srinivasan, A. Ruina, Computer optimization of a minimal biped model discovers walking and running. *Nature* **439**, 72–75 (2006).
11. M. Ackermann, A. J. Van Den Bogert, Optimality principles for model-based prediction of human gait. *J. Biomech.* **43**, 1055–1060 (2010).
12. M. Srinivasan, Fifteen observations on the structure of energy minimizing gaits in many simple biped models. *J. R. Soc. Interfac.* **8**, 74–98 (2011).
13. R. H. Miller, B. R. Umberger, J. Hamill, G. E. Caldwell, Evaluation of the minimum energy hypothesis and other potential optimality criteria for human running. *Proc. Biol. Sci.* **279**, 1498–1505 (2012).
14. V. Joshi, M. Srinivasan, Walking on a moving surface: Energy-optimal walking motions on a shaky bridge and a shaking treadmill can reduce energy costs below normal. *Proc. Roy. Soc. A* **471**, 20140662 (2015).
15. A. Falisse *et al.*, Rapid predictive simulations with complex musculoskeletal models suggest that diverse healthy and pathological human gaits can emerge from similar control strategies. *J. R. Soc. Interface* **16**, 20190402 (2019).
16. C. Dias, O. Ejtemai, M. Sarvi, N. Shiwakoti, Pedestrian walking characteristics through angled corridors: An experimental study. *Transport. Res. Rec.* **2421**, 41–50 (2014).
17. K. Mombaur, A. Truong, J.-P. Laumond, From human to humanoid locomotion: An inverse optimal control approach. *Aut. Robots* **28**, 369–383 (2010).
18. Q. Pham, H. Hicheur, G. Arechavaleta, J. Laumond, A. Berthoz, The formation of trajectories during goal-oriented locomotion in humans. II. A maximum smoothness model. *Eur. J. Neur.* **26**, 2391–2403 (2007).
19. G. Arechavaleta, J. Laumond, H. Hiceur, A. Berthoz, An optimality principle governing human walking. *IEEE Trans. Robot.* **24**, 5–14 (2008).
20. J. M. Brockway, Derivation of formulae used to calculate energy expenditure in man. *Hum. Nutr. Clin. Nutr.* **41C**, 463–471 (1987).
21. A. C. Bobbert, Energy expenditure in level and grade walking. *J. Appl. Physiol.* **15**, 1015–1021 (1960).
22. A. A. Neath, J. E. Cavanaugh, The Bayesian information criterion: Background, derivation, and applications. *Wiley Interdis. Rev. Comput. Stat.* **4**, 199–203 (2012).
23. M. Srinivasan, Optimal speeds for walking and running, and walking on a moving walkway. *Chaos* **19**, 026112 (2009).
24. M. S. Orendurff *et al.*, The kinematics and kinetics of turning: Limb asymmetries associated with walking a circular path. *Gait Posture* **23**, 106–111 (2006).
25. R. W. Bohannon, A. W. Andrews, Normal walking speed: A descriptive meta-analysis. *Physiotherapy* **97**, 182–189 (2011).
26. G. Arechavaleta, J.-P. Laumond, H. Hicheur, A. Berthoz, "The nonholonomic nature of human locomotion: A modeling study" in *The First IEEE/RAS-EMBS International Conference on Biomedical Robotics and Biomechatronics, 2006. BioRob 2006* (IEEE, Piscataway, NJ, 2006), pp. 158–163.
27. J. I. Neimark, N. A. Fufaev, *Dynamics of Nonholonomic Systems* (Translations of Mathematical Monographs, American Mathematical Society, Providence, RI, 1972), vol. 33.
28. H. Hicheur, Q. Pham, G. Arechavaleta, J. Laumond, A. Berthoz, The formation of trajectories during goal-oriented locomotion in humans. i. a stereotyped behaviour. *Eur. J. Neur.* **26**, 2376–2390 (2007).
29. J. J. Fruin, *Pedestrian Planning and Design* (Revised Edition, Elevator World, Inc., Mobile, AL, 1987).
30. M. N. Sreenivasa, I. Frissen, J. L. Souman, M. O. Ernst, Walking along curved paths of different angles: The relationship between head and trunk turning. *Exp. Brain Res.* **191**, 313–320 (2008).
31. P. Vivani, T. Flash, Minimum-jerk model, two-thirds power law, and isochrony: Converging approaches to movement planning. *J. Exp. Psychol. Hum. Percept. Perform.* **21**, 32–53 (1995).
32. J. D. Wong, T. Cluff, A. D. Kuo, The energetic basis for smooth human arm movements. bioRxiv [Preprint] (2020). https://doi.org/10.1101/2020.12.28.424067 (Accessed 1 February 2021).
33. R. Kram, Muscular force or work: What determines the metabolic energy cost of running. *Exerc. Sport Sci. Rev.* **28**, 138–143 (2000).
34. J. Doke, M. J. Donelan, A. D. Kuo, Mechanics and energetics of swinging the human leg. *J. Exp. Biol.* **208**, 439–445 (2005).
35. S. C. Miff, D. S. Childress, S. A. Gard, M. R. Meier, A. H. Hansen. Temporal symmetries during gait initiation and termination in nondisabled ambulators and in people with unilateral transtibial limb loss. *J. Rehabil. Res. Dev.* **42**, 175–182 (2005).
36. P. R. Greene, Running on flat turns: Experiments, theory, and applications. *J. Biomech. Eng.* **107**, 96 (1985).
37. Y.-H. Chang, R. Kram, Limitations to maximum running speed on flat curves. *J. Exp. Biol.* **210**, 971–982 (2007).
38. T. M. Griffin, T. J. Roberts, R. Kram, Metabolic cost of generating muscular force in human walking: Insights from load-carrying and speed experiments. *J. Appl. Physiol.* **95**, 172–183 (2003).
39. T. J. Roberts, R. Kram, P. G. Weyand, C. R. Taylor, Energetics of bipedal running. I. Metabolic cost of generating force. *J. Exp. Biol.* **201**, 2745–2751 (1998).
40. T. Y. Hubel, J. R. Usherwood, Children and adults minimise activated muscle volume by selecting gait parameters that balance gross mechanical power and work demands. *J. Exp. Biol.* **218**, 2830–2839 (2015).
41. A. A. Biewener, C. T. Farley, T. J. Roberts, M. Temaner, Muscle mechanical advantage of human walking and running: Implications for energy cost. *J. Appl. Physiol.* **97**, 2266–2274 (2004).
42. J. M. Donelan, R. Kram, The effect of reduced gravity on the kinematics of human walking: A test of the dynamic similarity hypothesis for locomotion. *J. Exp. Biol.* **200**, 3193–3201 (1997).
43. A. Grabowski, C. T. Farley, R. Kram, Independent metabolic costs of supporting body weight and accelerating body mass during walking. *J. Appl. Physiol.* **98**, 579–583 (2005).
44. M. Qiao, B. Brown, D. L. Jindrich, Compensations for increased rotational inertia during human cutting turns. *J. Exp. Biol.* **217**, 432–443 (2014).
45. G. Courtine, M. Schieppati, Human walking along a curved path. II. Gait features and EMG patterns. *Eur. J. Neur.* **18**, 191–205 (2003).
46. A. M. Turcato, M. Godi, A. Giordano, M. Schieppati, A. Nardone, The generation of centripetal force when walking in a circle: Insight from the distribution of ground reaction forces recorded by plantar insoles. *J. NeuroEng. Rehabil.* **12**, 4 (2015).
47. R. H. Miller, A comparison of muscle energy models for simulating human walking in three dimensions. *J. Biomech.* **47**, 1373–1381 (2014).
48. M. L. Handford, M. Srinivasan, Robotic lower limb prosthesis design through simultaneous computer optimizations of human and prosthesis costs. *Sci. Rep.* **6**, 19983 (2016).
49. C. O. Saglam, K. Byl, "Quantifying the trade-offs between stability versus energy use for underactuated biped walking" in *2014 IEEE/RSJ International Conference on Intelligent Robots and Systems* (IEEE, Piscataway, NJ, 2014), pp. 2550–2557.

50. N. Seethapathi, M. Srinivasan, Step-to-step variations in human running reveal how humans run without falling. *Elife* **8**, e38371 (2019).
51. V. Joshi, M. Srinivasan, A controller for walking derived from how humans recover from perturbations. *J. R. Soc. Interface* **16**, 20190027 (2019).
52. E. M. Summerside, R. Kram, A. A. Ahmed, Contributions of metabolic and temporal costs to human gait selection. *J. R. Soc. Interface* **15**, 20180197 (2018).
53. K. P. Körding, D. M. Wolpert, Bayesian integration in sensorimotor learning. *Nature* **427**, 244–247 (2004).
54. J. C. Selinger, S. M. O. Connor, J. D. Wong, J. M. Donelan, Humans can continuously optimize energetic cost during walking. *Curr. Biol.* **25**, 2452–2456 (2015).
55. J. D. Wong, S. M. O. Connor, J. C. Selinger, J. M. Donelan, Contribution of blood oxygen and carbon dioxide sensing to the energetic optimization of human walking. *J. Neurophysiol.* **118**, 1425–1433 (2017).
56. V. Edvardsen, A. Bicanski, N. Burgess, Navigating with grid and place cells in cluttered environments. *Hippocampus* **30**, 220–232 (2020).
57. W. H. Warren, B. R. Fajen, "Behavioral dynamics of visually guided locomotion" in *Coordination: Neural, Behavioral and Social Dynamics*, A. Fuchs, V. K. Jirsa, Eds. (Springer, Berlin, Heidelberg, 2008), pp. 45–75 (2008).
58. B. A. Baxter, W. H. Warren, Route selection in barrier avoidance. *Gait & Posture* **80**, 192–198 (2020).
59. R. Sedgeman, P. Goldie, R. Iansek, "Development of a measure of turning during walking" in *Advancing Rehabilitation Conference Proceedings* (La Trobe University, Melbourne, Australia, 1994), pp. 26–31.
60. M. A. Daley, A. J. Channon, G. S. Nolan, J. Hall, Preferred gait and walk–run transition speeds in ostriches measured using GPS-IMU sensors. *J. Exp. Biol.* **219**, 3301–3308 (2016).
61. J. C. Selinger, J. M. Donelan, Estimating instantaneous energetic cost during non-steady-state gait. *J. Appl. Physiol.* **117**, 1406–1415 (2014).
62. J. Zhang *et al.*, Human-in-the-loop optimization of exoskeleton assistance during walking. *Science* **356**, 1280–1284 (2017).

Supplementary Information and Figures for "A unified energy optimality criterion predicts human navigation paths and speeds"

Geoffrey L. Brown,[1,2,†] Nidhi Seethapathi,[1,3,†] Manoj Srinivasan[1,4,*]

[1]Mechanical and Aerospace Engineering, the Ohio State University, Columbus, OH 43210
[2]Feinberg School of Medicine, Northwestern University, Chicago, IL 60611
[3]Department of Bioengineering, University of Pennsylvania, Philadelphia, PA 19104
[4]Program in Biophysics, the Ohio State University, Columbus, OH 43210

[*]To whom correspondence should be addressed; E-mail: srinivasan.88@osu.edu.
[†]Equal contribution.

S1 Optimization methods for behavioral predictions for human path planning

As noted, we use numerical trajectory optimization techniques [1, 2] to determine the energy optimal solutions in Figures 4-6 of the main manuscript, for tasks that require determining the paths as well as speeds during walking. Here, we provide further technical details.

Optimal path between two points with end-point body orientations

This section corresponds to Figures 4-6 of the main manuscript, in which the goal is go from A to B, with constraints on the initial and final body orientation and, in some cases, velocities. To perform the trajectory optimization, we use the following multiple shooting approach [1]. We consider two kinds of models: non-holonomic and holonomic [3]. In the following, we use the terms 'velocity direction' and 'tangent to the path' interchangeably as they are identical.

Non-holonomic: always facing the movement direction

We parameterize the trajectory of the body continuously with N_{path} grid points, equally spaced in time. Each grid point has the following unknowns representing body state: $(x_b, y_b, \theta_b, v_b, \omega_b)$.

Here, x_b and y_b describe the body trajectory's top view (projection onto the horizontal plane), $v_b = \sqrt{\dot{x}_b^2 + \dot{y}_b^2}$ is the linear speed tangential to the trajectory, θ_b is both the body orientation and the velocity's angle with the x axis (so that $\dot{x}_b = v_b \cos\theta_b$ and $\dot{y}_b = v_b \sin\theta_b$ due to the non-holonomic constraint), and $\omega_b = \dot{\theta}_b$. The total time T_{path} is also an unknown.

Holonomic: not always facing the movement direction

We parameterize the trajectory of the body continuously with N_{path} grid points, equally spaced in time. Each grid point has the following unknowns representing body state:
$(x_b, y_b, \theta_b, v_{xb}, v_{yb}, \omega_b)$. Here, x_b and y_b describe the body trajectory's top view (projection onto the horizontal plane), $v_{xb} = \dot{x}_b$ and $v_{yb} = \dot{y}_b$ are the horizontal velocity components, θ_b is the body angular orientation but need not be aligned with the velocity direction (path tangent). The body angular velocity is $\omega_b = \dot{\theta}_b$. The total time T_{path} is also an unknown.

Multiple shooting and constraints

The following applies to both holonomic and non-holonomic settings, except that for the non-holonomic setting, we have $v_{xb} = v_b \cos\theta_b$ and $v_{yb} = v_b \sin\theta_b$ and for the holonomic setting, v_{xb} and v_{yb} are optimization unknowns. Starting from the i^{th} grid point (x_i, y_i, θ_i) with $i < N_{\text{path}}$, we integrate the following equations $\dot{x} = v_{xb}$, $\dot{y} = v_{yb}$, and $\dot{\theta} = \omega$, with v and ω considered (piecewise) linear, for each time duration $T_{\text{path}}/(N_{\text{path}} - 1)$. Then, we enforce the continuity constraints at the grid points by equating the end state of the integration to the state at the next grid point. We have constraints on the initial values of the body position and body orientation for all comparisons in Figures 4-6. In addition, for predicting the task in Mombaur et al, we constrain the initial body velocity to zero. For predicting Dias et al, we constrain the initial velocity while entering the corridor to energy-optimal straight line walking speed $v_{\text{opt}} = \sqrt{\alpha_0/\alpha_1}$, but leaving this initial velocity as an unknown to be determined by the optimization does not change the results. For predicting Arachavaleta et al, we leave the initial velocity as an unknown to be determined by the optimization, but constraining it to straight line optimal speed as above does not change the results. Body accelerations are limited to maximum values observed during walking [4]. For predicting Dias et al and Arachavaleta et al, we constrain the body trajectory (which corresponds to body center) to be at least a certain distance from the corridor corner or doors, respectively. This clearance value was chosen to be 0.35 based on typical human body dimensions [5]. We minimize the cost function subject to these constraints using nonlinear programming (`fmincon` in `MATLAB`).

Metabolic cost function

To compute the energy cost of the walk, we first compute the integral of the steady state metabolic rate over the path, using the appropriate metabolic rate expression for non-holonomic ($\dot{E} = \alpha_0' + \alpha_1' v_b^2 + \alpha_2' \omega^2$) and holonomic ($\dot{E} = \alpha_0' + \alpha_1' v_f^2 + \alpha_2' \omega^2 + \alpha_s v_s^2$). Here, v_f and v_s are components of the velocity along and perpendicular to the direction that the body faces. For

the Arachavaleta et al predictions, we add the cost of an additional 2 meters beyond point B to compute the total energy cost. To add an additional cost for changing speeds, we first compute the kinetic energy in the horizontal plane. Then, we evaluate the cost of the kinetic energy fluctuations as b_1 times total positive work (kinetic energy increases) and b_2 times total negative work (kinetic energy decreases), where $b_1 = 4$ and $b_2 = 0.85$, corresponding to reciprocals of typical muscle efficiencies, with a multiplicative factor $\lambda = 0.67$ as determined by Seethapathi and Srinivasan [6].

Turning in an angled corridor

This section provides some additional information on the angled-corridors task from Dias et al. We consider angled corridors with turn angle β. The length of the corridors on either side of the intersection point is 5 m. The width of the corridors are 1.5 m. The person starts from one end of one corridor and needs to get to the end of the other corridor, having made the turn. The person starts and ends at the middle of the corridor, 0.75 m from the wall. All these constraints are based on the experiments from Dias et al [7], with which we compare our results. As noted earlier, we add wall clearance as an inequality constraint ensuring that the subject does not contact the wall or go too close to the wall.

Sensitivity bands: Computing walking velocities or trajectories within 1%, 2% or 5% of the energy optimal strategy

In this article, for every calculation of optimal walking, we also compute and plot walking trajectories or velocities that are within 1%, 2%, and/or 5% of the optimum. Here, we briefly describe how these bands are computed using 2% as a placeholder percentage. These computations usually involve solving additional optimization or search problems.

For walking in circles or turning in place (Figures 2 and 3 of the main manuscript), it is a univariate problem of just finding the optimal linear or angular velocity and then finding the appropriate 2% band around it. To compute the 2% band, we first compute the optimal linear or angular velocity and then perform two one-dimensional searches — one above and one below the optimal velocity — to determine the two velocities that have 1.02 times the optimal energy cost. These two velocities determine the 2% band. We found the bands for other percentages analogously.

For the 2% bands for the Arachavaleta et al trajectories (Supplementary Figure S4), for each optimization calculation, we performed at least two additional optimization calculations. These were trajectory optimization problems with all the constraints of the original trajectory optimization problems. In addition, we add a constraint that the energy cost should be 1.02 times the optimal value. Finally, instead of minimizing the energy cost function (as the energy cost value is already constrained), we determine trajectories that have the "least x values", "greatest x values", etc. – that is, minimize $\sum_{i=1}^{N_{\text{path}}} x_i^2$, maximize $\sum_{i=1}^{N_{\text{path}}} x_i^2$, maximize $\sum_{i=1}^{N_{\text{path}}} y_i^2$, etc. These produce trajectories that have the lowest x values (most leftward path on average), largest

x values (most rightward path on average), etc., subject to being 1.02 times the cost. To avoid local minima, when we minimize $\sum_{i=1}^{N_{\text{path}}} x_i^2$, we also constrain the x_i to be entirely to the left of the optimal path (lower in values than that of the optimal path). It is important to note that the trajectories thus obtained need not contain all trajectories within 2% of the cost – nor is it true that every trajectory within this band has a cost within 2% of the optimum. Nevertheless, the bands formed by these computed paths will contain most well-behaved paths within 2% of the optimum; the bands also give us a lower bound on how far paths the paths can be while being within 2% of the optimum energy cost. Thus, the bands give a sense of how flat the energy landscape is near the optimum. Such substantial flatness of the energy landscape – resulting in substantially different trajectories being close in energy costs – may also accommodate time-reversal asymmetry to and from goals [8].

For Mombar et al and Dias et al comparisons, again we generate bands by solving new trajectory optimization problems as above. While we could have solved the problem described in the previous paragraph, we solved different optimization problems based on the comparisons being made. For Dias et al, because the comparisons were for turning velocity, we simply obtained trajectories that minimizes or maximized $\sum v_i^2$ over the path, subject to the energy cost being 1.02 times the optimal cost. For Mombaur et al, we computed trajectories that minimized or maximized the time duration of the task for simplicity while being 1.02 times the optimal cost. For Mombaur et al, an alternative would have been to minimize or maximize maximize $\sum x_i^2$ or $\sum y_i^2$ or $\sum \theta_i^2$ to obtain individual bands for the three state variables being plotted.

In all the holonomic walking calculations, we allow the body orientation to be at most 90 degrees relative to the velocity direction, so that walking backward is ruled out. But backward walking can be allowed easily by having a different coefficient α_1 when $|\theta - \beta| > \pi/2$ based on backward walking metabolic cost (known to be higher than forward walking costs and would therefore not be selected except in rare cases).

Walking in circles

In the main manuscript, to make behavioral predictions about walking in circles, we assumed the non-holonomic form of the metabolic cost function: $\dot{E} = \alpha_0' + \alpha_1' v_b^2 + \alpha_2' \omega^2$, with $v_b = R_b\,\omega$. However, allowing holonomic walking, namely using $\dot{E} = \alpha_0' + \alpha_1' v_f^2 + \alpha_2' \omega^2 + \alpha_s v_s^2$, will result in non-holonomy being selected as optimal, that is, with the sideways velocity $v_s = 0$ or $\beta = \theta$. Thus, the assumption of non-holonomy is internally self-consistent in this case of steady walking in circles.

S2 Centripetal model: feet movement vs body movement

Consider the body center of mass (mass m) moving in a horizontal circle with tangential speed v_b and radius R_b. Then, the legs need to not only support the body weight mg, but also the centripetal force mv_b^2/R_b, where g is acceleration due to gravity. Thus, the effective leg force is

oriented at an angle $\gamma = \tan^{-1}(v_b^2/R_b g)$ to the vertical. That is, the leg should be slanted inward. This standard simple model has been described [9]. This means that the foot travels in a slightly bigger circle than the body. The foot travel radius is then given by $R = R_b + \ell \sin\gamma$, where ℓ is the leg length. Further, if the average velocity of the effective foot is v, we have $v/R = v_b/R_b$ as the body and the feet go around their circles in the same time duration ($\omega = \omega_b$). Thus, we have the following three equations:

$$\frac{v}{R} = \frac{v_b}{R_b}, \quad \gamma = \tan^{-1}\frac{v_b^2}{gR_b}, \text{ and } \quad R_b = R - \ell\sin\gamma. \tag{1}$$

Given v, R, g, ℓ, we can compute the corresponding v_b, R_b and γ from these three equations. This calculation assumes that the two feet may travel along the same and that the (massless) leg always supports the body.

Our walking-in-circles metabolic experiments constrained the paths that the feet travel on rather than the paths that the body travels in. The original metabolic rate model was in terms of the foot travel variables v and R. We converted these to the corresponding body travel variables v_b and R_b and determined the best fit coefficients for $\dot{E} = \alpha_0' + \alpha_1' v_b^2 + \alpha_2' \omega_b^2$. We obtain the coefficient values to be $\alpha_0' = 2.32$ W/kg, $\alpha_1' = 1.28$ W/kg/$(\text{ms}^{-1})^2$, and $\alpha_2' = 1.02$ W/kg/$(\text{rad.s}^{-1})^2$. These coefficients were chosen to ensure that the optimal speeds for straight line walking and turning in place are the same as when computed with the foot-based cost landscape ($\alpha_0/\alpha_1 = \alpha_0'/\alpha_1'$ and $\alpha_0/\alpha_2 = \alpha_0'/\alpha_2'$). This best fit model explained approximately the same fraction of the metabolic cost data variance as the original metabolic model (about 87.5%), and so has about the same explanatory power as the foot-variables based metabolic cost model.

S3 Biomechanical reasons for the cost of turning

Why does walking with turning cost more energy than walking in a straight line? To be clear, none of our behavioral predictions and explanations of diverse behavioral data rely on mechanistically understanding the sources of the turning cost. Nevertheless, in this paragraph, we briefly consider a few mechanisms.

First, we consider the simplified cost due to centripetal forces described above. From elementary mechanics, we know that while walking in a circle, the body not only experiences gravity, but also centripetal acceleration. This centripetal acceleration is given by $a_n = v_b^2/R_\text{b}$, where v_b is the average body speed and R_b is the radius of the circle described by the body [9]. So, the legs need to provide the centripetal forces in addition to supporting body weight. Given that gravity is vertical and the centripetal acceleration is horizontal, as a first approximation, walking in circles might be viewed as walking under a slightly higher gravity equal to the total acceleration magnitude, namely $\sqrt{g^2 + a_n^2}$. However, for a speed of 1.6 m/s, radius $R = 1$ m, and $g = 9.81$ ms^{-2}, the acceleration magnitude $\sqrt{g^2 + a_n^2}$ is greater than gravity g only by about 1.3%. This increase in the 'effective gravity' and the corresponding leg force increase is too small to plausible affect the cost by nearly 50%.

Second, from scaling arguments and small angle approximations [1], it can be shown that similarly low incremental cost for turning is obtained if we consider a simplified point-mass model walking like a 3D inverted pendulum and using a metabolic cost proportional to leg mechanical work and/or leg force. This is because both the mechanical work and the leg force scale approximately with this effective gravity for these simple biped models [1].

As a third simple cost mechanism, we consider that the body is not a point-mass but consists of rigid body segments. The body, as a whole, not only moves in a circle, but also rotates by 360 degrees about the vertical axis. The average angular velocity ω of the body, treated as a single rigid body, is equal to the revolution rate $\omega = v/R$ of going around the circle. However, this body angular velocity fluctuates substantially within a stride between $\omega_{\min}$ and $\omega_{\max}$. We computed these body angular velocity fluctuations by using marker-based motion capture for six subjects as they walked in circles of different radii and lap durations (Figure S8). Assuming that these body angular velocity fluctuations require additional mechanical work, we derive an additional energy cost of about $0.1\,\omega^2$ in W/kg, if ω is in rad/s. This estimate is obtained by assuming a body moment of inertia $I_z = 2$ kgm^2 and mass $m = 70$ kg. When $\omega_{\max} > \omega_{\min} > 0$, both the positive and negative work per cycle equal $I_z(\omega_{\max}^2 - \omega_{\min}^2)/2$; when $\omega_{\max} > 0$ and $\omega_{\min} < 0$, both the positive and negative work per cycle equal $I_z(\omega_{\max}^2 + \omega_{\min}^2)/2$. Then, the metabolic cost per stride is estimated as $b_1 = 4$ times positive work and $b_2 = 0.85$ times negative work, where again, b_1 and b_2 are reciprocals of muscle efficiencies. Then, the metabolic cost per time is estimated by dividing by the stride period, also estimated from the motion capture data.

Thus, the costs predicted from simple models is still an order of magnitude smaller than the $0.96\,\omega^2$ obtained in experiment (equation 1 of the main manuscript). Thus, we conclude that an explanation of the additional metabolic cost may require a more detailed model of the human body, for instance, one that better models the body kinematics, the musculature and the muscle metabolic rate, which is well beyond the scope of this article. We reiterate that none of this has any effect on our behavioral predictions and their agreement with data.

S4 Why smoothness-only objectives predict infinitesimal movement speeds and how speeds scale with distance

We noted in the main manuscript that *pure* smoothness-related objectives [10, 11] such as related to acceleration and its first or second derivatives (termed 'jerk' or 'snap') predict infinitesimal velocities in the absence of additional cost terms. Here, we provide mathematical intuition for why such objectives predict infinitesimal speeds, well-known in the reaching literature [12]. For instance, consider the acceleration based cost:

$$J_a = \int_0^T \dot{v}^2 \, dt$$

or a jerk-based cost

$$J_j = \int_0^T \dddot{v}^2 \, dt$$

for a task that requires you to go from A to B in a straight line, separated by distance D. Consider an optimal solution for the position $x_1(t)$ for some given fixed time duration T_1, so that $x_1(0) = 0$ and $x_1(T) = D$. We now show that the cost can be lower for a longer time duration T_2 (that is, $T_2 > T_1$). To show this, consider a new motion $x_2(t) = x_1(tT_2/T_1)$, so that $x_2(0) = 0$ and $x_2(T_2) = D$. This new motion $x_2(t)$ is a slowed down (time-stretched) version of $x_1(t)$. So we can write both motions in terms of a single function $g(p)$ with $0 \leq p \leq 1$, so that:

$$x_1(t) = g(p) \text{ with } p = t/T_1$$

and

$$x_2(t) = g(p) \text{ with } p = t/T_2.$$

Given that $\ddot{x}_1 = (d^2g/dp^2) \cdot (1/T_1)^2$ and $x_2(t)$ is analogous, we can write the respective acceleration costs as:

$$J_{a1} = \int_0^{T_1} \ddot{x}_1(t)^2 dt = \int_0^1 \left(\frac{d^2g}{dp^2}\right)^2 \frac{1}{T_1^4} T_1 dp = \int_0^1 \left(\frac{d^2g}{dp^2}\right)^2 \frac{1}{T_1^3} dp$$

and

$$J_{a2} = \int_0^1 \left(\frac{d^2g}{dp^2}\right)^2 \frac{1}{T_2^3} dp.$$

Thus, $J_{a2} < J_{a1}$ if $T_2 > T_1$, so that driving duration T to zero is optimal, so infinitesimal speeds are best. Similarly, the jerk cost J_j will be given by

$$J_j = \int_0^1 \left(\frac{d^3g}{dp^3}\right)^2 \frac{1}{T^5} dp,$$

make the inverse dependence on duration only starker, so again infinitesimal speeds are optimal. Further, this general result of infinitesimal speeds being optimal does not rely on the exponent being 2 on the cost integrand; it works for any exponent greater than 1 for both jerk and acceleration costs.

Sometimes, this non-ecological speed prediction is avoided by having a cost for time, equivalent to having an additive constant inside the integrand, for instance in [3], as:

$$\int_0^T (c_0 + c_1 \dot{v}^2) dt \text{ or } \int_0^T (c_0 + c_1 \ddot{v}^2) dt.$$

Because of the c_0, the integral has an additional term $c_0 T$, because of which, infinitesimal speed and infinite duration becomes non-optimal and finite duration becomes optimal. However, this fix introduces new issues as it makes the optimal speed quite dependent on the distance

traveled (unless the functional form of the cost is carefully contrived), much more than seen in experiment. For simplicity, define $g(p) = D \cdot h(p)$ in the above reasoning, so that the same overall trajectory $h(p)$ is scaled in both space and time to obtain any particular distance and time. Then, the total acceleration cost will be:

$$c_0 T + \frac{D^2}{T^3} c_3$$

where c_3 is the integral $\int h''(p)^2 dp$. Minimizing this quantity with respect to T makes the time duration scale with $\sqrt{D}$, so that speed $v = D/T \sim D/\sqrt{D} \sim \sqrt{D}$. Locomotor speeds do not scale like this with distance [6]. As a consequence, we predict that the cost expression obtained in [3] will predict larger and larger walking velocities for larger and larger distances (well beyond human capability). It can be verified that using jerk cost version produces an even worse dependence of speed on distance ($v \sim D^{0.6\bar{6}}$). However, minimizing a velocity dependent cost (as we have used)

$$\int (c_0 + c_1 v^\gamma) dt$$

for walking a given distance D ensures that the optimal duration T is proportional to D, so that the optimal velocity v is independent of distance D, as expected.

We have made these arguments in the context of straight line motion, but having analogous terms for angular motion, for instance, ω and its derivatives results analogous qualitative conclusions regarding turning.

Of course, as noted in the main manuscript, the real objective function may contain acceleration or jerk-related cost terms (perhaps as a proxy for force rate costs) in addition to a velocity dependent costs that we have used. Our critique of these smoothness costs is primarily in their use to the exclusion of metabolic-like costs.

Model	Bayes Information Criterion	R-squared value
Default: $\alpha_0 + \alpha_1 v^2 + \alpha_2 \omega^2$	48.20	88.05
$\ldots + \alpha_3 v$	52.86	88.06
$\ldots + \alpha_4 \lvert\omega\rvert$	50.84	88.28
$\ldots + \alpha_5 v \lvert\omega\rvert$	52.50	88.10
$\ldots + \alpha_3 v + \alpha_4 \lvert\omega\rvert$	55.33	88.30
$\ldots + \alpha_3 v + \alpha_5 v \lvert\omega\rvert$	52.09	88.64
$\ldots + \alpha_4 \lvert\omega\rvert + \alpha_5 v \lvert\omega\rvert$	57.13	88.10
$\ldots + \alpha_3 v + \alpha_4 \lvert\omega\rvert + \alpha_5 v \lvert\omega\rvert$	55.78	88.75

Table S1: The default model, namely, $\alpha_0 + \alpha_1 v^2 + \alpha_2 \omega^2$, has the lowest Bayesian Information Criterion (BIC). Picking the model with the lowest BIC allows us to pick a model does not overfit the data, while penalizing model complexity (ie., promoting parsimony). BIC is equivalent to cross-validation procedures asymptotically for linear models [13]. Moreover, we see using a general quadratic relation with six coefficients increases the fraction of variance explained (R-squared value) by less than 0.7%. Recall that we use the absolute value $|\omega|$ here because we did not distinguish between left and right turns in our experiments or analyses, and assume the metabolic rate to be an even function in ω.

References

[1] M. Srinivasan, Fifteen observations on the structure of energy minimizing gaits in many simple biped models. *J. R. Soc. Interface* **8**, 74-98 (2011).

[2] J. T. Betts, *Practical Methods for Optimal Control Using Nonlinear Programming* (SIAM, 2001).

[3] K. Mombaur, A. Truong, J.-P. Laumond, From human to humanoid locomotionan inverse optimal control approach. *Auton. Robots* **28**, 369–383 (2010).

[4] S. C. Miff, D. S. Childress, S. A. Gard, M. R. Meier, A. H. Hansen, Temporal symmetries during gait initiation and termination in nondisabled ambulators and in people with unilateral transtibial limb loss. *Journal of Rehabilitation Research & Development* **42** (2005).

[5] J. Fruin, *Pedestrian Planning and Design, Revised Edition* (Elevator World, Inc., Alabama, 1987).

[6] N. Seethapathi, M. Srinivasan, The metabolic cost of changing walking speeds is significant, implies lower optimal speeds for shorter distances, and increases daily energy estimates. *Biol. Letters* **11**, 20150486 (2015).

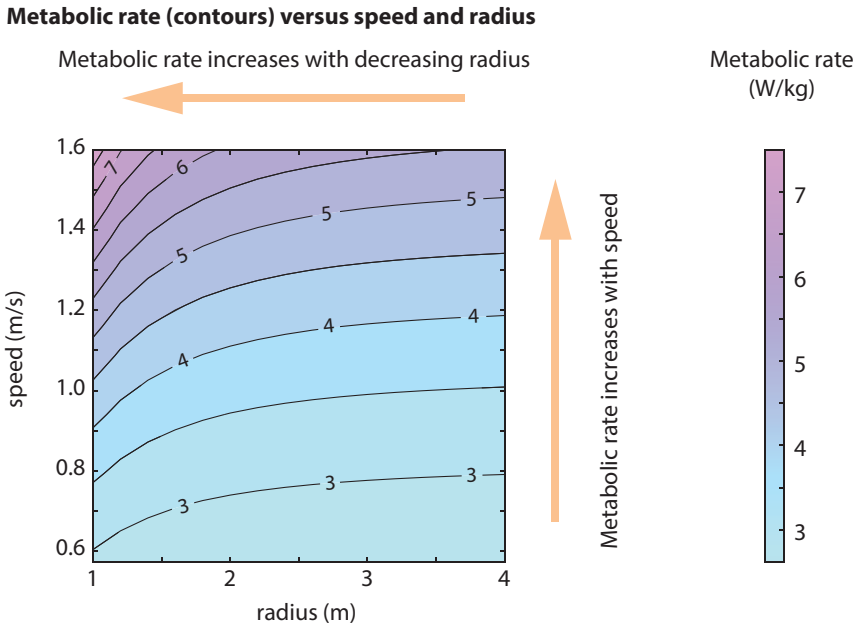

Figure S1: Metabolic rate contours. In Figure 1b of the main manuscript, we showed a 3D surface plot of the metabolic rate versus tangential speed and radius. Here, we show a 2D contour plot of the same surface, given by equation 1. The metabolic rate increases with speed for any fixed radius and it increases for decreasing radius for a given speed.

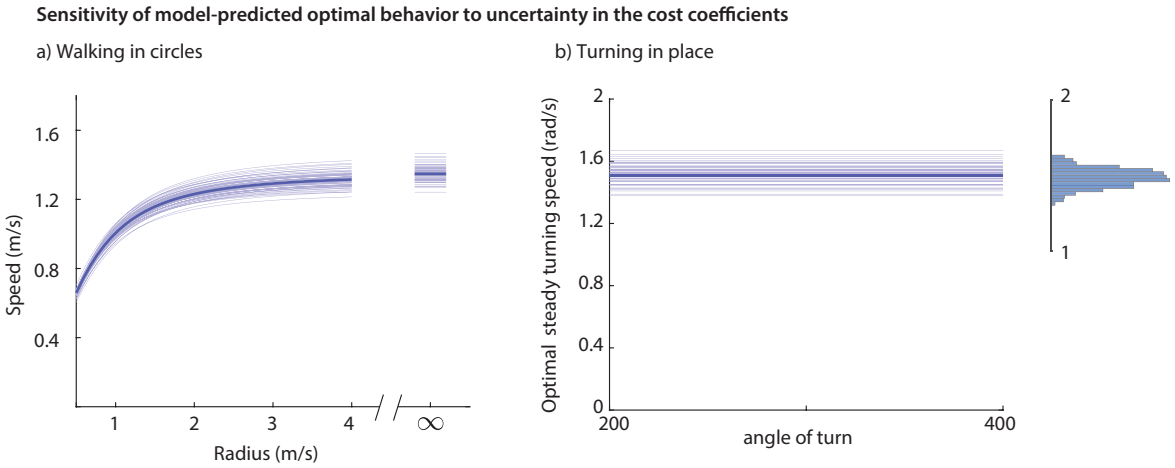

Figure S2: Optimal walking in circles: Prediction sensitivity to coefficient uncertainty. Parts a and b of this figure are analogous to Figures 2B and 3C of the main manuscript, respectively. To produce the different curves, we sampled 50 sets of coefficients α_0, α_1, α_2 at random from a normally distributed probability distribution that reflects the uncertainty in these coefficients: this multivariate normal distribution has mean coefficient values used in the main manuscript and covariance equal to the error covariance of the estimated coefficients. The error covariance of the coefficients was obtained using `fitlm` in MATLAB. For each set of coefficients, we computed the preferred walking speeds in circles and preferred steady angular speeds of turning in place, as in the main manuscript, to produce these plots. We note that these optima lie well within the blue bands in the main manuscript, which signify the set of speeds within 1-5% of the optimal speeds.

[7] C. Dias, O. Ejtemai, M. Sarvi, N. Shiwakoti, Pedestrian walking characteristics through angled corridors: An experimental study. *Transportation research record* **2421**, 41–50 (2014).

[8] M. Sreenivasa, K. Mombaur, J.-P. Laumond, Walking paths to and from a goal differ: on the role of bearing angle in the formation of human locomotion paths. *Plos one* **10**, e0121714 (2015).

[9] P. R. Greene, Running on flat turns: experiments, theory, and applications. *J. Biomech. Eng.* **107**, 96 (1985).

[10] Q. Pham, H. Hicheur, G. Arechavaleta, J. Laumond, A. Berthoz, The formation of trajectories during goal-oriented locomotion in humans. ii. a maximum smoothness model. *Eur. J. Neur.* **26**, 2391-2403 (2007).

[11] G. Arechavaleta, J. Laumond, H. Hiceur, A. Berthoz, An optimality principle governing human walking. *IEEE Trans. Robots* **24**, 5-14 (2008).

[12] P. Vivani, T. Flash, Minimum-jerk model, two-thirds power law, and isochrony: converging approaches to movement planning. *Journal of Experimental Psychology: Human Perception and Performance* **21**, 32-53 (1995).

[13] J. Shao, An asymptotic theory for linear model selection. *Statistica sinica* pp. 221–242 (1997).

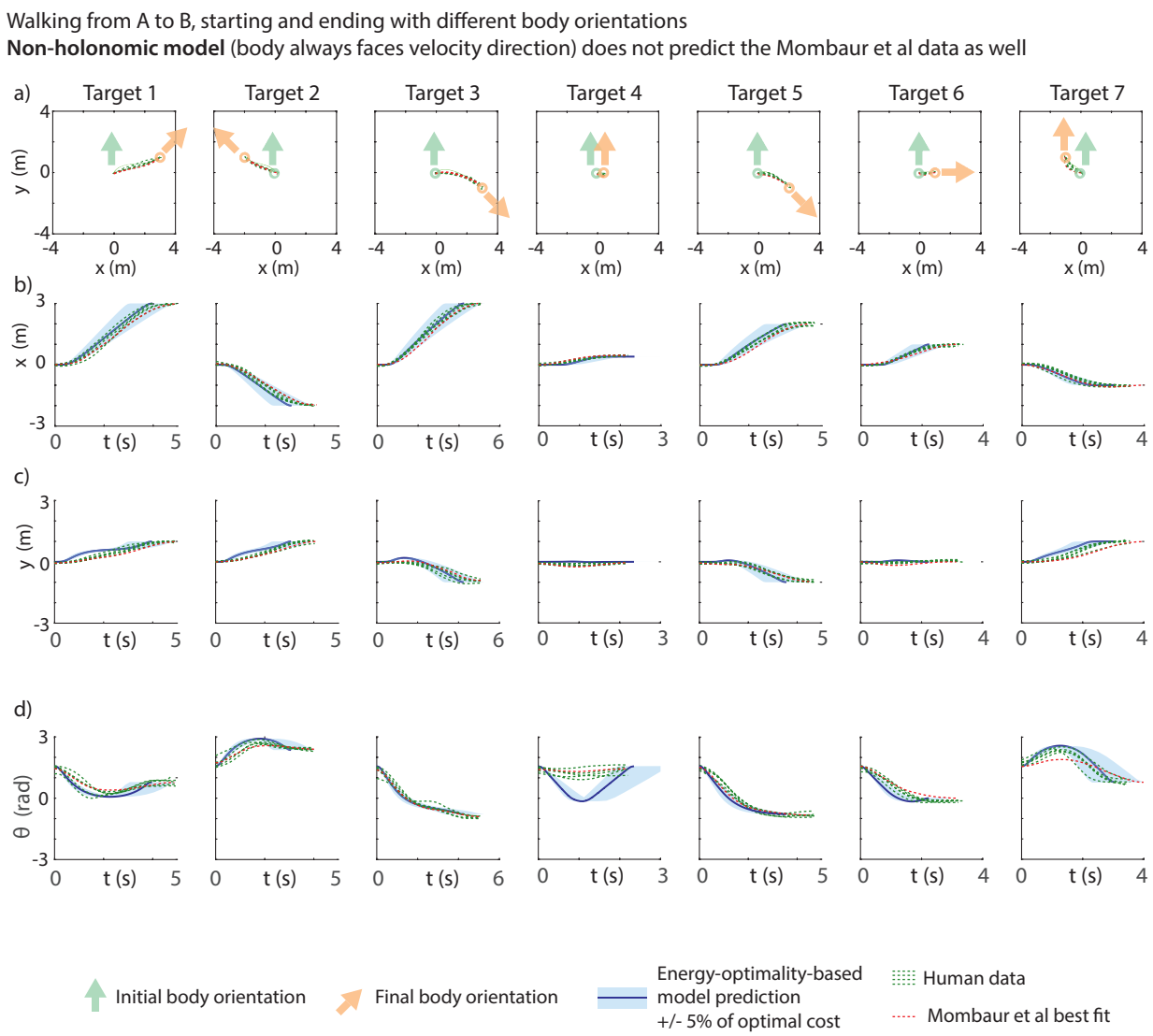

Figure S3: Prediction vs behavior: Predicting path planning via a non-holonomic model. a) Mombaur et al [3] asked subjects to walk short distances, starting at rest at point A and ending at rest at point B. The subjects had to start facing one direction (light green arrow) and end facing possibly another direction (orange arrow). b, c, d) The body position (x, y) and body orientation θ as a function of time. The only difference with the corresponding figure in the main manuscript is that the predictions are based on non-holonomic walking assumptions (facing always in the movement direction). Non-holonomic model predictions are solid dark blue with a light blue band indicating trajectories withing 5% of the optimum cost; experimental data are dashed dark green, and the best-fit model in Mombaur et al [3] is indicated in dashed red line. We see that these non-holonomic model predictions do not agree with data as well as holonomic model predictions in the main manuscript.

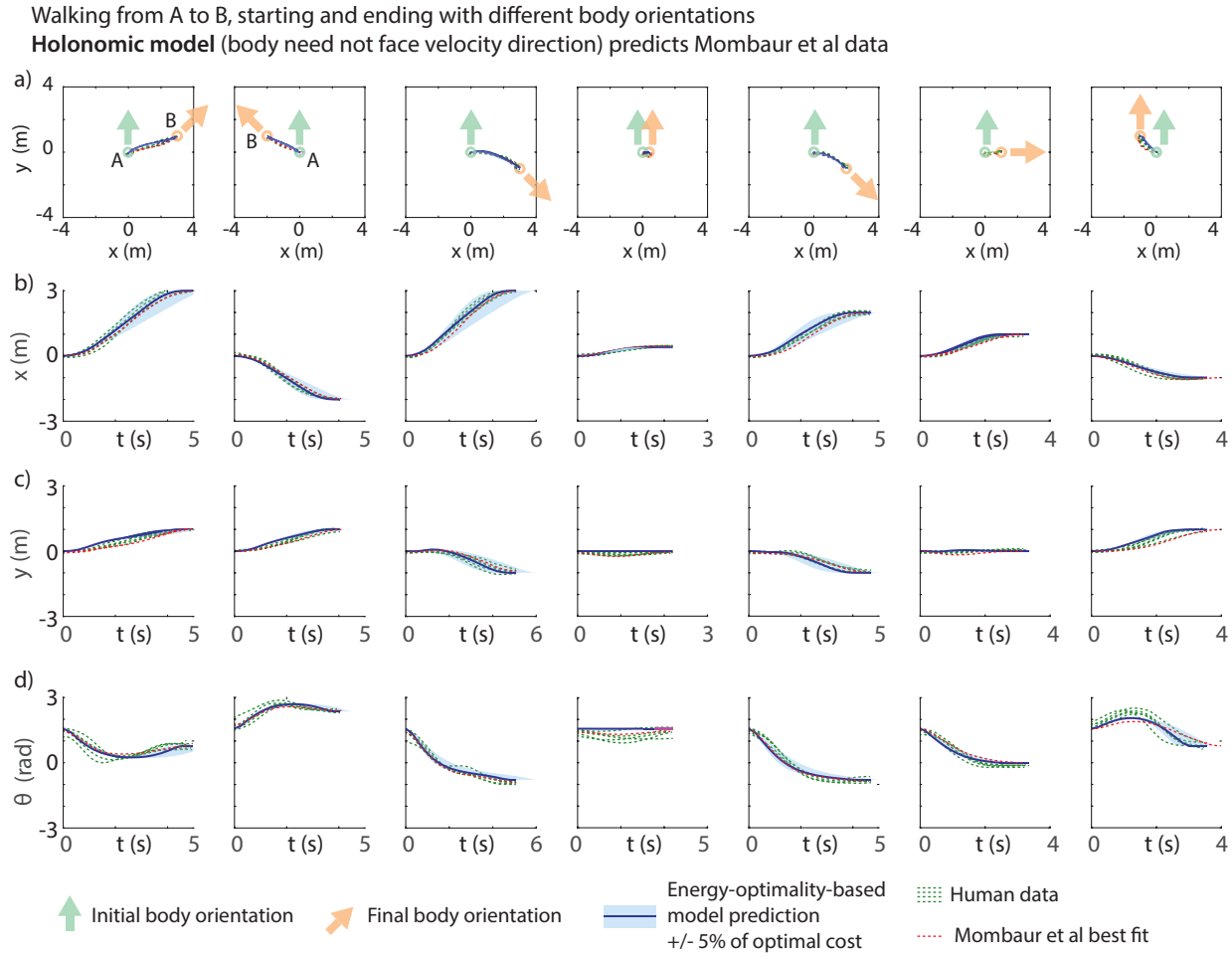

Figure S4: Prediction vs behavior: Predicting path planning via a holonomic model. This figure is identical to the corresponding figure in the main manuscript, except for what the initial and final body orientation conditions for the optimization. In the main manuscript, for targets 4 and 7, we used the initial and final body orientation conditions equal to what the subjects started and ended at on average. Here instead, we use the initial and final body orientation conditions equal to that prescribed by the experimenter. Of course, the results of the optimization are very similar to that in the main manuscript except for these small differences – and still predict the observed experimental data well.

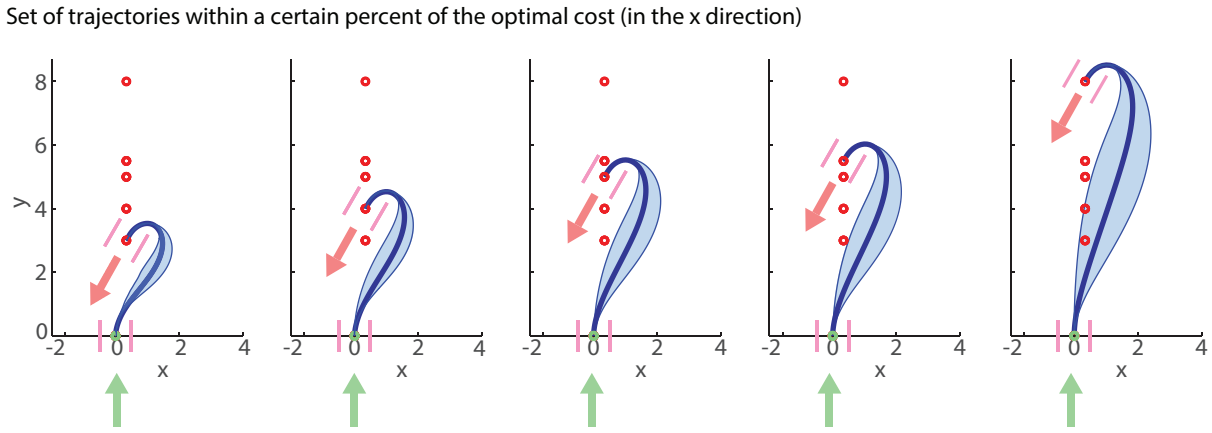

Figure S5: Path planning via two doorways. These figures complement the comparison figures for data from Arachavaleta et al in the main manuscript, except now, we show light blue bands around the optimal trajectories. These light blue bands indicate sets of trajectories that are within 2% of the optimal energy costs, in the sense described in the body of this Appendix. We note that the human trajectories are within these bands.

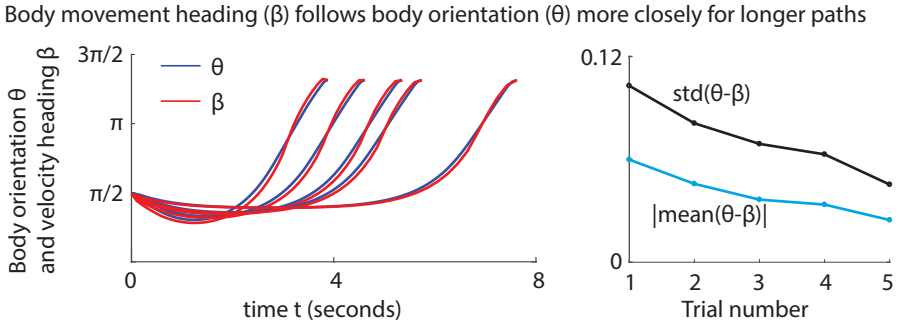

Figure S6: Body movement heading follows body orientation more closely for longer paths. a) We show how closely movement direction β follows body orientation θ for the optimal holonomic paths for the five different trials in Figure 6 of the main manuscript (tasks from Arachavaleta et al, as above). b) Mean and standard deviation of the difference between the two orientations decreases with the distance between the initial point and final point. In this plot, the x-axis denotes trial number, with the shortest trial labeled trial 1 and the longest trial labeled trial 5.

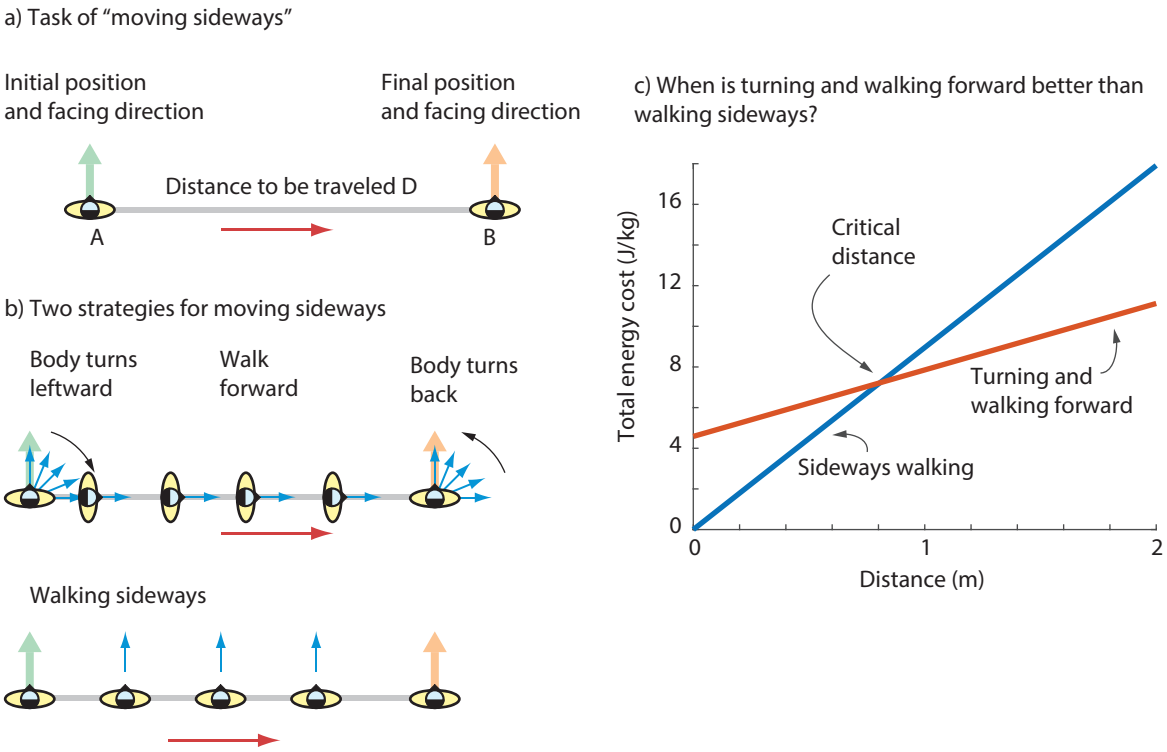

Figure S7: Stepping sideways vs turning and walking forward. a) Consider a task in which a human needs to go from A to B, starting and ending facing perpendicular to the line AB. b) Two strategies: sideways walking versus turning and walking forward. c) Metabolic comparison of the two strategies shows a transition in behavior at a critical distance. Indeed, target 4 of the Mombaur et al data is close to this task with $D = 0.4$ and subjects essentially step sideways without much of turning rightward, consistent with the prediction.

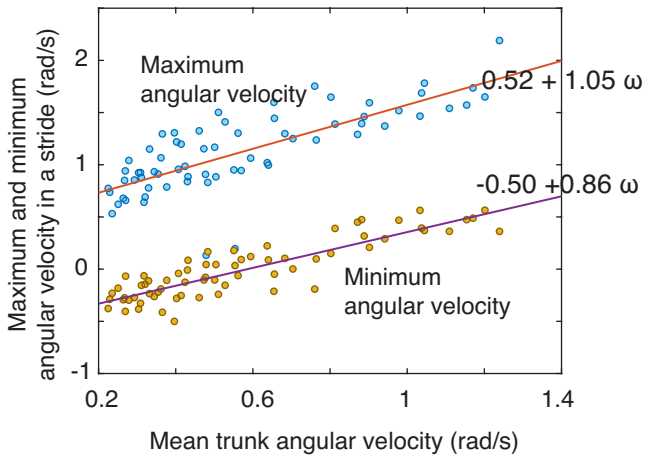

Figure S8: Trunk angular velocity fluctuations. While walking in circles, the trunk angular velocity fluctuates about the mean angular velocity ω. Here, the maximum and minimum of such fluctuations are plotted against the mean for 4 radii and at least 4 speeds for all subjects. We see that the fluctuations retain a roughly constant range, slightly increasing with ω.